Journal of the Atmospheric Sciences

Collision fluctuations of lucky droplets with superdroplets

--Manuscript Draft--

Manuscript Number:	JAS-D-20-0371
Full Title:	Collision fluctuations of lucky droplets with superdroplets
Article Type:	Article
Corresponding Author:	Xiang-Yu Li Pacific Northwest National Laboratory Richland, WA UNITED STATES
Corresponding Author's Institution:	Pacific Northwest National Laboratory
First Author:	Xiang-Yu Li
Order of Authors:	Xiang-Yu Li
	Bernhard Mehlig
	Gunilla Svensson
	Axel Brandenburg
	Nils Haugen
Abstract:	It was previously shown that the superdroplet algorithm to model the collision-coalescence process can faithfully represent mean droplet growth in turbulent aerosols. But an open question is how accurately the superdroplet algorithm accounts for fluctuations in the collisional aggregation process. Such fluctuations are particularly important in dilute suspensions. Even in the absence of turbulence, Poisson fluctuations of collision times in dilute suspensions may result in substantial variations in the growth process, resulting in a broad distribution of growth times to reach a certain droplet size. We quantify the accuracy of the superdroplet algorithm in describing the fluctuating growth history of a larger droplet that settles under the effect of gravity in a quiescent fluid and collides with a dilute suspension of smaller droplets that were initially randomly distributed in space (‘lucky droplet model’). We assess the effect of fluctuations upon the growth history of the lucky droplet and compute the distribution of cumulative collision times. The latter is shown to be sensitive enough to detect the subtle increase of fluctuations associated with collisions between multiple lucky droplets. The superdroplet algorithm incorporates fluctuations in two distinct ways: through the random distribution of superdroplets and through the explicit Monte Carlo algorithm involved when two superdroplets reside within the volume around one mesh point. Through specifically designed numerical experiments, we show that both sources of fluctuations on their own give an accurate representation of fluctuations. We conclude that the superdroplet algorithm can faithfully represent fluctuations in the coagulation of droplets driven by gravity.

We thank the reviewers for their repeated evaluation of our manuscript.
We have addressed all points, as detailed below. The resulting changes
in the manuscript are marked in blue.

> Reviewer #1
> Review of "Collision fluctuations of lucky droplets with superdroplets"
> by Xiang-Yu Li et al. In response to my previous comments, the poor
> narrative of the manuscript has been improved a little bit, but not
> satisfactory yet. In addition, there is a growing concern regarding
> the numerical setup of this study, which could substantially affect
> the main conclusions; that is, the height of the domain for approach IV
> (both 1-D and 3-D) could be too small. In this revised manuscript, the
> authors provide more detail about their numerical setup, and as a
result,
> the issue has come to the surface. I would suggest the authors rerun
all
> the simulations with a much taller domain. If not, the authors have to
> clearly justify that it is not crucial for this study. I acknowledge
> that this is a cutting edge study. It is worth publishing, but after
> all these issues are resolved.

We have now modified the code so that we can run many realizations in one
run. In this way, we have now demonstrated that the results are
insensitive
to the domain size and also the density of background droplets;
see our changes to the paper in section 4.a.

> Major Comments
> 1) [request] P. 8, Eq. (7)
> It is still unclear whether multiplicity \xi_i is an integer or a
> real number in this study. Please clarify how you calculate \xi_i/2
> and \xi_j/2 in Eq. (7) when \xi_i/2=\xi_j/2 is an odd number.

In the paragraph below that of Eq.(7), we have now added the following to
clarify that \xi is a real number in our study: "We emphasize that Eq.
(5)
does not require \xi to be an integer. Since we usually specify the
initial number density of physical particles, \xi may well be fractional
from the beginning. This is different from the integer treatment of \xi
in Shima et al 2009."

> 2) [request] P. 8, ll. 159--161, "It is then assumed that, ..."
> I do not understand. Does "two superdroplets with less than
> one physical droplet" mean \xi_i<1 \wedge \xi_j<1? How can such
> superdroplets be created from Eqs. (5) and (7)? Could you elaborate?

We have now explained that \xi can be any fractional number already
initially, thus Eq.(5) does not pose any constraint on this.

> 3) [question] P. 11, ll. 213--215, 1-D setup I have several questions
> regarding the setup. You explain that n_0=3e8 m^{-3}. Please clarify
if
> n_0 includes the lucky droplet or not. You distributed 256 droplets
> in the domain. Then, the number concentration including the lucky

> droplets is 256/8.56\times10^{-7}\unit{m^{3}}\approx2.99\unit{m^{-3},
> and the number concentration of background droplets is
> 255/8.56\times10^{-7}\unit{m^{3}}\approx2.98\unit{m^{-3}; both are
> slightly smaller than n_0. Is this difference acceptable?

We have now written "initial number density of background droplets
of...".
Instead of giving both the volume and the side lengths, we give just the side lengths of the domain. We now see that we were not accurate enough in specifying those, but we judge that this <1% error does not affect our results in any visible way.

> 4) [question] P. 11, ll. 216 and 218, time step Please add the units.
> Here, you show a fixed time step, but on p. 7, l. 134, you said that
> it is adaptively determined. Which is correct?

We have now rephrased our statement as the following,
"...are integrated with an adaptive time step, the mean value
of which delta t = 2.94 x 10^{-4} s.

> 5) [request] P. 11, ll. 219, "Ngrid=64"
> Please clarify the shape of the grid used for the 3-D simulations.
> 4x4x4, 2x2x16, or anything else?

We now write that "we use a cubic mesh with 4^3 points".

> 6) [request] P. 12, l. 221, "125 collisions are required" This is
> not correct. 123 collisions are required for a lucky droplet with
> an initial radius 12.6 um grow to 50 um.

We agree with the referee and have now corrected this. This mistake was also done in the earlier papers, which we have now emphasized in the text.

> 7) [suggestion] P. 11, ll. 221, "This justifies our use of Ns(t0)>=128"
> In both 1-D and 3-D, the vertical extent of the domains are too small
> and not appropriate for the purpose of the study.
> In 1-D, you have only 255 background droplets in the domain. Then, at
> the time when the lucky droplet grows to 50 um, the number of
background
> droplets reduces from 255 to 132. Therefore, the number concentration
of
> the background droplets reduces from 2.98 m^{-3} to 1.54 m^{-3}, i.e.,
> almost halved! However, in the original LDM (approach I) it is assumed
> that is constant in time. Considering that the lucky droplet falls
> about 100 m or much more, we can expect that the substantial decrease
> of n^{back} has a strong impact on the results.

The number of superdroplets is kept approximately constant, i.e., for this experiment, only a negligible fraction of background droplets are removed from the simulations. We say this now in the middle of paragraph 6 of Sec.4.a. Whether or not this compromises the statistical accuracy is now being addressed in the new Figure 8, where we also address other potential shortcomings pointed out by the referee below. We have now also

conducted simulations with larger sizes (2L, 8L, and 64L) and showed in Fig.8(c) that P(T) is insensitive to the domain size. Therefore, the size we chose is appropriate for this study.

Also, we demonstrated that P(T) is insensitive to xi, as discussed in section A2, "The most practical application of the superdroplet algorithm is the case when xi^i > 1. Thus, we investigate how xi affects fluctuations by performing the same 1-D simulation as described in section 2.b with different values of xi^i(t0). Fig.A1(b) shows that P(T) is insensitive to xi^i(t0), which suggests that the superdroplet algorithm can capture the effects of fluctuations regardless of the value of xi^i(t0)."

> In 3-D, the setup is more confusing to me. I assumed that the shape of
> the grid is 2x2x16. Then, in the column where the lucky superdroplet
> is located, you have only 64 droplets (32 superdroplets) in it on
> average. This is not at all sufficient for the lucky droplet to grow
> to 50 um, because 64 is much less than 123x2 (x2 is for the two lucky
> droplets). Am I missing something?

We recall that the boundary condition for the superdroplets is periodic and that the number of droplets is approximately constant. This is how 50 um is reached in our simulations. We have clarified this now in the text in the 5th paragraph of Section 4.a.

> All in all, I strongly suggest the authors rerun all the simulations
> in much taller domains, say 100m, to obtain reliable statistics. For
> taller domains, I consider the difference between 1-D and 3-D will
> become negligible. If the authors stick to their original numerical
> setup, they at least have to provide some clear justification of their
> numerical setup.

We have now added a new Figure 8 to clarify quantitatively the shortcomings of different tallness of the domain and different densities. We hope that the discussion around our new Figure 8 clarifies these questions. In our approach II, our domain is actually large enough and background particles are not recycled. In approach IV, we show that there is no marked difference compared with a 64 times larger domain.

> 8) [request] P. 12, l. 230, "After the kth collision step ..." This
> is not correct, because the initial size of the lucky droplet is . You
> may say "After (k-2)th collision step ..." or add a note "For
> convenience, we consider k starts from 3.". Please make it rigorous.

We have corrected it to (k-1)th, because after the first collision means after r2 has collided with r1, so k-1=1=first.

> 9) [request] P. 12, Eq. (9)
> This must be a summation from k=3 to 125, not k=2 to 125. Please
correct.

We agree that there is a problem, but according to our counting, the first
collision must happen with the lucky droplet of radius r2=12.6um, so the

first mean waiting time is t2 = ...*(r2+r1)^2 (v2-v1). The first collision
leads to r3. The target radius 50um is r_125, and it is achieved by colliding
with a droplet of radius r_124, so the sum should go from k=2 to 124.

> 10) [request] P. 12, l. 124, "124 collisions" Not "124 collisions"
> but "123 collisions".

We have corrected this now.

> 11) [request] P. 12, Eq. (10)
> This is something that I already pointed out in (9) of my previous
> review comments, but this equation and the explanation that follows
> are incorrect. Here is my suggestion how to introduce lambda_k: The collision
> rate at the (k+1)th collision of the lucky droplet r_k obeys lambda_k=...,
> where E_k=..., and v_k and v_1 are given by their terminal velocities.
> Note here that lambda_k is the collision rate between the lucky droplets
> and ALL the background droplets, therefore lambda_k /= lambda_k1. To
> avoid this confusion, I suggest you not use the greek letter lambda
> for lambda_k. In relation to the above note, how do you evaluate the
> velocities of the droplets in approach I? I assume that you use their
> terminal velocity. Please clarify this point.

Yes, we do use the terminal velocities here. (We have checked at one point that the inclusion of the acceleration phase made virtually no difference.) We have now included the formulation suggested by the referee.

> 12) [request] P. 13, ll. 251--252, "Given that the variance of ..."
> This is again what I already pointed out in my previous comment (10). You
> should explicitly mention that the variance of the mean collision time
> is lambda_k^{-2}. Otherwise, readers cannot tell if the variance is
> large for smaller k.

We have adopted this formulation in the revised text after Eq.(11).

> 13) [comment] P. 13, Eq. (12)
> Here you assumed the terminal velocity.

Yes, and this is now explained in our response to your earlier point above.
We made this assumption in Sect.3d (page 17) when we solve a dynamical model, but we felt it would be confusing to make a corresponding remark at this point, where we just state the cross section as a function of a given velocity difference.

> 14) [request] P. 13, l. 261, "... would correspond to the expression
> equation (4) used in the superdroplet algorithm" Eq. (12) does not
> correspond to Eq. (4), but corresponds to Eq. (10). Please correct.

We have now corrected this.

> 15) [request and suggestions] P. 14, l. 277, "In Figure 4 ..." In
> Figure 4, you are comparing not P(T) but the normalized probability
> density, P(T/<T>). Please explicitly mention this here. As you show in
> Table 2, <T> differs very much among the three cases. <T> is an
important
> quantity that characterizes the behavior of the lucky droplet. Why do
you
> compare not P(T) but P(T/<T>)? Please explain. I do not say comparing
> P(T/<T>) is pointless, but I strongly suggest that you should discuss
> the difference of <T> as well.

We have now added an extra paragraph emphasizing this; see the
penultimate
paragraph of Section 3.b.

> 16) [request] P. 15, l. 288, "In Figure 5, ..." The same as the above
> applies here. According to Table 2, <T> differs very much among the
three
> cases. Please explain why you compare not P(T) but P(T/<T>). Please
also
> discuss the difference of <T>.

This applies actually to all our plots of distribution times, and was
also done in the work of Kostinski and Shaw.

> 17) [comment] P. 15, l. 302, "it does not result in any significant
> error to assume r_k >> r_1" I do not agree. According to Table 2, <T>
> are different among the three cases in Fig. 4. Please discuss this
point.

We agree with the referee and have now inserted "as far as the shapes
of the different curves is concerned" in that sentence; see the first
sentence of the third paragraph after Eq.(16). Regarding the changes
of <T>, we have now added an additional paragraph after the present
paragraph.

> 18) [request] P. 15, l. 306, "T_125^MFT".
> Based on the definition (14), <T>=T_124^MFT. Please show this relation
> to the readers and provide the values of T_124^MFT", not T_125^MFT".

We agree with the referee, so we have now added the sentence "We normally
compute <T> as an average over all realizations, but these averages
also agree with T_124^MFT." Regarding the variation, we have now added
"On the other hand, the actual averages such as $<T> ~ T_124^MFT vary
by almost 50%."

> 19) [request] P. 18, l. 351, approach III
> You have to explain explicitly that you will use only two superdroplets
in
> approach III; one for the lucky droplet and the other for the
background

> droplets. Please also clarify whether you remove the background droplet
> (i.e., decrease the multiplicity) after coalescence or not. This is
> important information because lambda_k is proportional to the
multiplicity of
> the background superdroplet, and hence lambda_k changes in time if you
remove
> the background droplet. Please also specify the size of the domain you
> use for approach III. If you do not remove background droplets and the
> background droplet number concentration is unchanged, I understand that
> the domain size does not matter to approach III. If it is the case,
please
> explain this explicitly in the manuscript to increase the readability.

We have done this now added the sentence "We note that in this approach, n is kept constant, i.e., no background droplet is being removed after a collision."

> 20) [request] P. 19, l. 393, "We see examples in Figure 8 ..."
> Is this approach IV in 1-D? Please clarify.

Yes. We have added this now to the caption of Figure 6, but not to that of Figure 8, because it says "same as Figure 6". In addition, in the caption
to Figure 11 we have now added that it is done with approach III.

> 21) [request and question] P. 20, l. 403, "approach III"
> Please explicitly explain that you have one superdroplet that
represents
> the background droplets. When the collision-coalescence of two lucky
> droplets takes place, do you remove one of the lucky droplets? Please
> clarify.

To clarify this, we have now added the parenthetic sentence "(As always in approach III, the background particles are still represented by only one superdroplet, and n is kept constant.)"

> 22) [question] P. 20, Eq. (19)
> Is epsilon only for approach III? In approach III, are all N_d^luck,
> N_d^back, xi_i, N_s^luck, and N_d^back constant in time? If not, please
> declare that you define epsilon by their initial value.

Yes, epsilon is an input parameter only for approach III, but we also estimate its effective value for approach IV, when we discuss Figure 6. We have now also clarified this by adding the parenthetic sentence "(In that approach, all quantities in Eq.(19) are kept constant.)"

> 23) [request] P. 20, l. 413, "in the full superdroplet model studied
> above, ..." Do you mean "in the full superdroplet model studied in
> Fig. 8, ..."? Please clarify where you are pointing.

We have now added "(see Figures 6 and 9)" in parentheses.

> 24) [request] P. 21, l. 426, "As shown in section 4.b, ..." We are
> still in Sec. 4.b. Please clarify.

We have now removed "As shown in section 4.b", because we do already refer to Figure 11 in this sentence.

> 25) [request] P. 21, l. 431, "Figure 11"
> Is this a result of approach III? Please clarify.

Yes, this have now been added in the caption.

> 26) [question] P. 22, l. 450, "..., thus containing on average 700
> droplets." Because the number concentration of the background droplets
> is 3e8 m^{-3}, is it not 2100 droplets on average? Anyway, the domain is much
> taller than that in approach IV. I believe you should test approach IV
> (1-D and 3-D) in a similarly sized domain.

We agree with the referee regarding 2100 droplets on average and have now corrected this. The results for taller domains are shown in our new Figure 8.

> 27) [question] P. 22, l. 459, "..., we could only run 10^3
> realizations." I do not understand why the computational cost of
> approach IV is much larger than other approaches. Could you provide some
> explanation why?

This is because we solve the momentum equation (Eq.1) of all the superdroplets
and detect their collision. So the time step is determined by the smallest value
between the Stokes time and the collision time, which is often quite small and
therefore the time step is small.
Also, in the original calculation, every
single simulation was treated as a separate run, and poor usage of the parallelization was made. We have now added an option to the Pencil Code to run independent realizations all in one go, which allowed us now to present results for the 8192 realizations in our new Figure 8.

> 28) [request] P. 23, l. 466, "4-d. The effect of fluctuations in 3-D
> simulations" I think the fluctuations in 3-D in your simulation is very
> much exaggerated because the domain is not tall enough. Please rerun the
> simulations with a much taller domain or provide some concrete evidence
> that the domain height for 1-D and 3-D is not crucial.

The effect of fluctuations agrees with what we expect theoretically. While
we agree that the domain was not tall enough for accurate results, especially for the correct representation of rare events, we emphasize that effect of lateral fluctuations has the opposite trend and that therefore, these two effects compensate each other.

> 29) [request] P. 4, ll. 79--80, "The ratio of droplets per

> superdroplet is called the multiplicity." This explanation is not
> precise enough. I would suggest the following: "The number of droplets
> in each superdroplet is called the multiplicity."

We have now changed it to "The number of droplets in each superdroplet
is called the multiplicity."

> 30) [typo] P. 5, l. 104, "Third"
> I could not find any "First" or "Second".

We have now removed the "Third" and rephrased the sentence,
"As the small ..."

> 31) [request] P. 7, ll. 131--132, "To avoid a probability larger than
> unity, we limit the integration step through the condition ..." Shima
> et al. (2009) introduced the multiple coalescence trick to relax this
> condition. Unterstrasser et al. (2020) confirmed that this technique
> works efficiently. Please explicitly mention that this is not adopted
> in this study.

We explicitly explained this at the end of section 2.a in the first
revised version. We have now elaborated more on it as the following,
"To reduce the computational cost and make it linear in the number of
superdroplets per mesh point, n_s(t), Shima et al. (2009) assumed that
each droplet interacts at most with one other one, which is referred
to as random permutation technique. This technique was also adopted in
Dziekan and Pawlowska (2017) and Unterstrasser et al. (2020) but is not
used in the Pencil Code ..."

> 32) [request] P. 9, ll. 163--164, "..., Shima et al. (2009) assumed
> that ..." This is not precise because it is not an assumption. I would
> suggest the following: "..., Shima et al. (2009) imposed that ..."

We have now replaced "assumed" by "imposed".

> 33) [typo] P. 9, ll. 165--166, "This technique was also..."
> Repetition. Please delete the second "Dziekan and Pawlowska (2017)".

We have now removed it.

> 34) [request] P. 9, ll. 175--176, "Since the flow is not disturbed
> by the particles, we neglect two-way coupling" This is a misleading
> statement. I understand that the flow is assumed to be quiescent and
> the time evolution of the flow is not calculated in this study. If I am
> correct, please remove the sentence.

We have now removed it.

> 35) [request] P. 10, l. 186, "... lucky and background droplets
> ..." This has to be "... lucky and background superdroplets ..."

We have now changed it to "superdroplets".

> 36) [typo] P. 12, l. 245, "collision rate (4)" Collision rate (10)

We have corrected this now.

> 37) [typo] P.14, l. 274, "In the right hand panel" Perhaps "In
> Fig. 2"?

We have now changed it to Fig.2.

> 38) [request] P. 14, l. 277
> Please explicitly explain that you are using the Approach I here.

We have now added "...using approach I".

> 39) [typo] P. 14, Eq. (16) Do you mean min(1,(r_k/r*)^2)? If so,
> please correct the following: "late in the evolution" -> "early in
> the evolution" (P. 14, l.285), "r_k>=r*" -> "r_k<=r*" (P. 14,
> l. 286).

No, the text is correct as it is; we really meant the late evolution. We wanted to say that P(T) is not only sensitive to the first few collisions, but *also* later collisions, (albeit to a lesser extent. To show this, we have used a modified form of E(r) such that E=const for r<r_*, but increasing quadratically for larger values. The form (r/r_*)^2 becomes zero for r -> 0, but to prevent this and to have a constant value, we clip it by using the max function.

> 40) [typo] P. 14, l. 286, "To ensure that E_k<=1, ... to ensure
> E_k<=1" Remove one of the two "to ensure that E_k<=1".

We have now removed one of them.

> 41) [typo] P. 15, l. 306 "Table 3" -> "Table 2"

We have now corrected it.

> 42) [request] P. 19, l. 378, "\int P(T) dT = 1" Ambiguous
> explanation. In Figure 7, are you showing P(T/<T>)=<T>P(T),
> the probability density of T/<T>? Please clarify.

We agree with the referee and have now omitted this. The P(T) or P(T/<T>) are of course normalized as earlier in the paper.

> 43) [typo] P. 52, Fig. 7. N_p/s is not defined.

We have corrected this and have replaced N_p/s by xi.

Reviewer #2

> Review of a revised manuscript "Collision fluctuations of lucky
> droplets with superdroplets" by Li at al. Recommendation: accept
> after additional revisions General comments: The revised manuscript has
> been improved. I like the expanded and now very comprehensive list of

> references to previous studies in both communities (i.e., astrophysics
> and cloud physics). However, I feel the lead author run simulations
> described in the paper by custom-adopting the DNS code he is using in
> other publications, the Pencil code. As far as I can tell there is no
> flow dynamics in the simulations (see line 516) and thus references to
> the Pencil code (and other related comments, see below) only provide
> confusion. I think this has to change to improve readability. Overall,
> the results are of interest and should be eventually published.
> Line-by-line comments:

It is true that there is no fluid dynamics in the present paper, but the superdroplet algorithm is part of the Pencil Code and this part has been used when working with approach IV. Any changes or improvements that we have made are publicly available in the default version of the code.

> 1. L. 116: Replace "in terms of" by "by".

It is now replaced.

> 2. L. 126-128: The following text is unclear: "When two superdroplets
> collide, a Monte-Carlo scheme is used to determine which pairs of
> superdroplets collide. All pairs of superdroplets within the volume
> around one mesh point may collide.". I suggest revising the description
> of the collision algorithm. Please see how other describe collisions of
> real droplets as represented by superdroplets.

We have now revised this text; see the blue part in the text above Equation (3).

> 3. L. 129: as above. What do you mean by "two droplets in either of
> the superdroplets"? I do not think separate droplet collisions are
> considered, superdroplet collisions are.

We have now changed it to "Superdroplet i and j residing in the same grid cell collide with a probability of ...".

>4. L. 133: Why does the speed of sound (and other factors) limit the
> time step? I think you mean in the dynamic model, but it is not used
> in simulations discussed in this paper. I suggest removal.

We have now removed it.

> 5. L. 168: What is the PENCIL CODE? If this is a dynamic model (like
> the DNS code), why it is referred to in this paper? As far as I can
> understand, there is no fluid flow in the simulations. See my general
> comment above.

We have now rephrased that part to explain that the Pencil Code comes with many different modules, many of which are not invoked in the present studies. The particle modules are part of the code, and that part is used in the present studies.

> 6. L. 193: "(One time step...". Why? I do not think this is
> correct. Maybe because of the coupling with the dynamic model, but the

> dynamic model is not used in the simulations.

We solve the momentum equation of particles (Eq.1 and Eq.2), where the Stokes time in Eq.(2) need to be resolved. Also the collision time scale,
which is the inverse of Eq.(4) should be resolved.

We have now explained it as follows: "The simulation time step must be less than the time for a superdroplet to fall from one mesh point to the next (Stokes time expressed in equation (2)) and the collision time scale (inverse of the collision rate expressed in equation (4))"

> 7. Paragraph starting at L. 211. I do not understand why the reference
> to the Pencil code is needed as there is no flow dynamics. The problem
> of droplet collisions can be solved without any grid. I think I miss
> something from the very beginning (see general comments). The 2 mm grid
> in x and y is unclear. Why only about 20 cm in the vertical? Similar
> comment for the 3D simulations. 3D does not have flow dynamics either,
> just nonuniform spatial droplet distribution, correct?

We already explained that the Pencil Code is not just a DNS code. The particle modules are part of it. It is true that droplet collisions can be
solved without a mesh, and this is done in approach II. The connection with a mesh is an essential aspect of the superdroplet approach and is explained in paragraph 3 of Section 2.a. It avoids the problem of searching for possible collision partners. As we emphasize in the paper, the superdroplet approach (which we also refer to as approach IV) is a combination between approaches II and III, and in approach III there are only two superdroplets. Those are at the same mesh point, so a mesh is needed even then, even though we only need one! We hope that our paper clarifies this aspect of the superdroplet approach of Shima et al, which was not discussed previously.

> 8. L. 242: what is "stopping time" for the collision?

We have now rephrased it and write: "Here we use the subscript k to represent the time until the kth collision."

> 9. Please use the same scales and labels on the axes in Fig.6 and 8.
> Please check other figures that the text calls to compare.

We have now applied the same scales and labels on the axes in Fig.6 and 8 and other figures.

Reviewer #3:

> Following up on the review of the JAS-D-20-0371, let me confirm that
> several updates carried out by the Authors made the paper read much
> better. I'm providing below a list of several minor issues still worth
> addressing in my opinion:

We thank the referee for the repeated review of our manuscript.

> 1. Earlier references on the lucky droplet model and related discussion
> worth citing, e.g.: Twomey 1964: "Statistical Effects in the Evolution
> of a Distribution of Cloud Droplets by Coalescence" Madival 2018:
> "Stochastic growth of cloud droplets by collisions during settling"

We have now cited these papers; see the third-to-last paragraph of the introduction.

> 2. On page 7/l138, the Authors rightly point out that superdroplets
> of the same size can never collide with a geometric kernel (4); it would
> be worth to elaborate as well on the issue of lack of representation of
> self-collisions within a single superdroplet. The point is that even with
> a collision kernel allowing collisions among droplets of the same size,
> the superdroplet algorithm does not feature collision of same-sized
> droplets within a single superdroplet.

We have now added the following below Eq.(4),
"Moreover, no collision is allowed in a single superdroplet"

> 3. p8/l159: in Shima et al., the multiplicities are represented with
> integer numbers, worth pointing out this difference.

We have now added the following below Eq.(7)
"Since we usually specify the initial number density of physical particles, \xi may well be fractional from the beginning. This is different from the integer treatment of \xi in Shima et al. (2009)."

> 4. p9/l168: the linearity of computational cost is worth elaborating on:
> as the Authors hint, it is the number of super-droplets per collision
> volume that has either quadratic or linear scaling; however, as the
> pair-sampling method can always be balanced by introducing substeps to
> obtain matching statistics, what is likely of greater importance is the
> lack of data dependence across candidate pairs in the Shima approach
> which paves the way for parallel evaluation. For discussion, see e.g.,
> section 2.3.3 in Unterstrasser et al. 2020, also Bartman & Arabas 2021)

The text in this paragraph, which was not well written, has now improved. In addition, we have added the following text to the end of the paragraph in order to be explicit about the parallelization:
"For the Pencil Code, collisions between particles residing within a given grid cell are evaluated by the same processor which is also evaluating the fluid equations of that grid cell. Due to this, together with the domain decomposition used in the code, the particle collisions are automatically efficiently parallelized as long as the particles are more or less uniformly distributed over the domain."

> 5. p15/l307 "four approaches" are mentioned before being defined.

We have now removed it.

> 6. Technical issues with references I have pointed out in previous
>   iteration were not addressed:
> - some reference entries include DOIs, some not;
> - several include doubled URLs (i.e., DOI and DOI-URL);
> - acronyms and proper names have bogus spelling (Mcsnow,
>   lagrangian, kuiper, slams, neptunian, lcm1d, warsaw, uwlcm, monte
carlo);
> - capitalisation is not consistent;
> - some journal names are abbreviated, some not.

We have now made all the references consistent. We apologize for overlooking this issue in the previous iteration.

Collision fluctuations of lucky droplets with superdroplets

Xiang-Yu Li[a, b, c, d], Bernhard Mehlig[e], Gunilla Svensson[a, c], Axel Brandenburg[b, d, f], Nils E. L. Haugen[g, h]

[a] *Department of Meteorology and Bolin Centre for Climate Research, Stockholm University, Stockholm, Sweden*

[b] *Nordita, KTH Royal Institute of Technology and Stockholm University, 10691 Stockholm, Sweden*

[c] *Swedish e-Science Research Centre, www.e-science.se, Stockholm, Sweden*

[d] *JILA and Laboratory for Atmospheric and Space Physics, University of Colorado, Boulder, CO 80303, USA*

[e] *Department of Physics, Gothenburg University, 41296 Gothenburg, Sweden*

[f] *Department of Astronomy, Stockholm University, SE-10691 Stockholm, Sweden*

[g] *SINTEF Energy Research, 7465 Trondheim, Norway*

[h] *Department of Energy and Process Engineering, NTNU, 7491 Trondheim, Norway*

Corresponding author: Xiang-Yu Li, xiang.yu.li@su.se, September 13, 2021, Revision: 1.715

ABSTRACT: It was previously shown that the superdroplet algorithm for modeling the collision-coalescence process can faithfully represent mean droplet growth in turbulent aerosols. But an open question is how accurately the superdroplet algorithm accounts for fluctuations in the collisional aggregation process. Such fluctuations are particularly important in dilute suspensions. Even in the absence of turbulence, Poisson fluctuations of collision times in dilute suspensions may result in substantial variations in the growth process, resulting in a broad distribution of growth times to reach a certain droplet size. We quantify the accuracy of the superdroplet algorithm in describing the fluctuating growth history of a larger droplet that settles under the effect of gravity in a quiescent fluid and collides with a dilute suspension of smaller droplets that were initially randomly distributed in space ('lucky droplet model'). We assess the effect of fluctuations upon the growth history of the lucky droplet and compute the distribution of cumulative collision times. The latter is shown to be sensitive enough to detect the subtle increase of fluctuations associated with collisions between multiple lucky droplets. The superdroplet algorithm incorporates fluctuations in two distinct ways: through the random distribution of superdroplets and through the explicit Monte Carlo algorithm involved when two superdroplets reside within the volume around one mesh point. Through specifically designed numerical experiments, we show that both sources of fluctuations on their own give an accurate representation of fluctuations. We conclude that the superdroplet algorithm can faithfully represent fluctuations in the coagulation of droplets driven by gravity.

1. Introduction

Direct numerical simulations (DNS) have become an essential tool to investigate collisional growth of droplets in turbulence (Onishi et al. 2015; Saito and Gotoh 2018). Here, DNS refers to the realistic modeling of all relevant processes, which involves not only the use of a realistic viscosity, but also a realistic modeling of collisions of droplet pairs in phase space. The most natural and physical way to analyze collisional growth is to track individual droplets and to record their collisions, one by one. However, DNS of the collision-coalescence process are very challenging, not only when a large number of droplets must be tracked, but also because the flow must be resolved over a large range of time and length scales.

Over the past few decades, an alternative way of modeling aerosols has gained popularity. Zannetti (1984) introduced the concept of "superparticles, i.e., simulation particles representing a cloud of physical particles having similar characteristics." This concept was also used by Paoli et al. (2004) in the context of condensation problems. The application to coagulation problems was pioneered by Zsom and Dullemond (2008) and Shima et al. (2009), who also developed a computationally efficient algorithm. The idea is to combine physical aerosol droplets into 'superdroplets'. To gain efficiency, one tracks only superdroplet collisions and uses a Monte Carlo algorithm (Sokal 1997) to account for collisions between physical droplets. The superdroplet algorithm is used in both the meteorological literature (Shima et al. 2009; Sölch and Kärcher 2010; Riechelmann et al. 2012; Arabas and Shima 2013; Naumann and Seifert 2015, 2016; Unterstrasser et al. 2017; Dziekan and Pawlowska 2017; Li et al. 2017, 2018, 2019, 2020; Sato et al. 2017; Jaruga and Pawlowska 2018; Brdar and Seifert 2018; Sato et al. 2018; Seifert et al. 2019; Hoffmann et al. 2019; Dziekan et al. 2019; Grabowski et al. 2019; Shima et al. 2020; Grabowski 2020; Unterstrasser et al. 2020), as well as in the astrophysical literature (Zsom and Dullemond 2008; Ormel et al. 2009; Zsom et al. 2010; Johansen et al. 2012; Johansen et al. 2015; Ros and Johansen 2013; Drakowska et al. 2014; Kobayashi et al. 2019; Baehr and Klahr 2019; Ros et al. 2019; Nesvorný et al. 2019; Yang and Zhu 2020; Poon et al. 2020; Li and Mattsson 2020; Li, X.-Y. and Mattsson, L. 2021). Compared with DNS, the superdroplet algorithm is distinctly more efficient. It has been shown to accurately model average properties of droplet growth in turbulent aerosols. Li et al. (2018) demonstrated, for example, that the mean collision rate obtained using the superdroplet algorithm

agrees with the mean turbulent collision rate (Saffman and Turner 1956) when the droplets are small.

Less is known about how the superdroplet algorithm represents fluctuations in the collisional aggregation process. Dziekan and Pawlowska (2017) compared the results of the superdroplet algorithm with the predictions of the stochastic coagulation equation of Gillespie (1972) in the context of coalescence of droplets settling in a quiescent fluid. Dziekan and Pawlowska (2017) concluded that the results of the superdroplet algorithm qualitatively agree with what Kostinski and Shaw (2005) called the lucky droplet model (LDM). To assess the importance of fluctuations, Dziekan and Pawlowska (2017) computed the time $t_{10\%}$, after which 10% of the droplets have reached a radius of $40\,\mu$m. In agreement with earlier Lagrangian simulations of Onishi et al. (2015), which did not employ the superdroplet algorithm, they found that the difference in $t_{10\%}$ between their superdroplet simulations and the stochastic model of (Gillespie 1972) decreases with the square root of the number of droplets, provided that there are no more than about nine droplets per superdroplet. The number of droplets in each superdroplet is called the multiplicity. When this number is larger than 9, they found that a residual error remains. We return to this question in the discussion of the present paper, where we tentatively associate their findings with the occurrence of several large (lucky) droplets that grew from the finite tail of their initial droplet distribution.

The role of fluctuations is particularly important in dilute systems, where rare extreme events may substantially broaden the droplet-size distribution. This is well captured by the LDM, which was first proposed by Telford (1955) and later numerically addressed by Twomey (1964), and more recently quantitatively analyzed by Kostinski and Shaw (2005). The model describes one large droplet (twice the mass of $10\,\mu$m-sized droplets in radius) settling through a dilute suspension of smaller droplets. The collision times between the larger droplets (the lucky droplet) and the smaller ones are exponentially distributed, leading to substantial fluctuations in the growth history of the lucky droplet. Wilkinson (2016) derived analytic expressions for the cumulative distribution times using large-deviation theory. Madival (2018) extended the theory of Kostinski and Shaw (2005) by considering a more general form of the droplet-size distribution than just the Poisson distribution.

The goal of the present paper is to investigate how accurately the superdroplet algorithm represents fluctuations in the collisional growth history of settling droplets in a quiescent fluid. Unlike the work of Dziekan and Pawlowska (2017), who focused on the calculation of $t_{10\%}$ we compare

here with the LDM. We record growth histories of the larger droplet in an ensemble of different realizations of identical smaller droplets that were initially randomly distributed in a quiescent fluid. We show that the superdroplet algorithm accurately describes the fluctuations of growth histories of the lucky droplet in an ensemble of simulations. In its simplest form, the LDM assumes that the lucky droplet is large compared to the background droplets, so that the radius of those smaller droplets can be neglected in the geometrical collision cross section and collision velocities. Since fluctuations early on in the growth history are most important (Kostinski and Shaw 2005; Wilkinson 2016), this can make a certain difference in the distribution of the time T it takes for the lucky droplet to grow to a certain size. As the small droplets are initially randomly distributed, their local number density fluctuates. Consequently, lucky droplets can grow most quickly where the local number density of small droplets happens to be large. This needs to be taken into account when comparing with three-dimensional (3-D) versions of the LDM.

The remainder of this paper is organized as follows. In section 2 we describe the superdroplet algorithm and highlight differences between different implementations used in the literature (Shima et al. 2009; Johansen et al. 2012; Li et al. 2017). Section 3 summarizes the LDM, the setup of our superdroplet simulations, and how we measure fluctuations of growth histories. Section 4 summarizes the results of our superdroplet simulations. We conclude in section 6.

2. Method

a. Superdroplet algorithm

Superdroplet algorithms represent several physical droplets by one superdroplet. All droplets in superdroplet i are assumed to have the same material density ρ_d, the same radius r_i, the same velocity $\boldsymbol{v}_i$, and reside in a volume around the same position $\boldsymbol{x}_i$. The index i labeling the superdroplets

TABLE 1. Definition of variables in superdroplet algorithm.

n	number density of droplets in the domain
n_luck	number density of lucky droplets
$N_\mathrm{s}(t)$	Number of "superdroplets" in the domain
$\xi_i(t)$	Number of droplets in superdroplet i (multiplicity)
$N_\mathrm{d}(t)$	Total number of physical droplets in the domain
N_real	number of independent simulations (realizations)

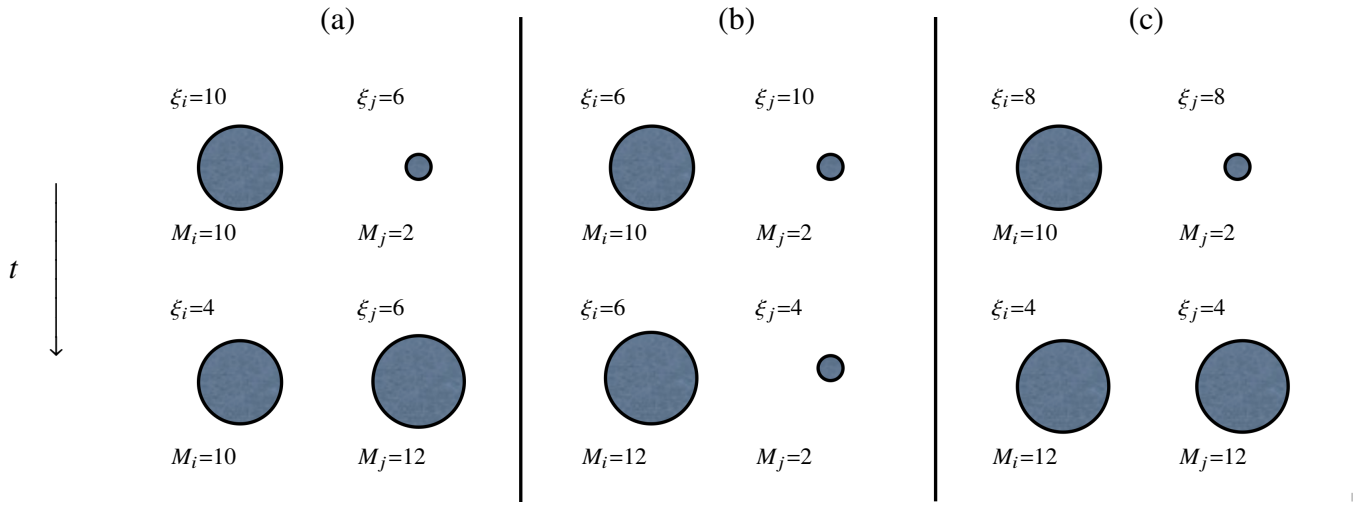

FIG. 1. Collision outcomes when two superdroplets collide and droplet collisions occur. Time increases downward, as indicated by the arrow. Superdroplet i contains ξ_i large droplets of mass M_i, superdroplet j contains ξ_j small droplets of mass $M_j < M_i$.

ranges from 1 to $N_\mathrm{s}(t_0)$ (Table 1), where t_0 denotes the initial time. The hydrodynamic force is modeled using Stokes law.

The equation of motion for the position $\boldsymbol{x}_i$ and velocity $\boldsymbol{v}_i$ of superdroplet i reads:

$$\frac{\mathrm{d}\boldsymbol{x}_i}{\mathrm{d}t} = \boldsymbol{v}_i\,, \quad \frac{\mathrm{d}\boldsymbol{v}_i}{\mathrm{d}t} = -\frac{\boldsymbol{v}_i}{\tau_i} + \boldsymbol{g}\,. \tag{1}$$

Here $\boldsymbol{g}$ is the gravitational acceleration,

$$\tau_i = \frac{2}{9}\frac{\rho_\mathrm{d}}{\rho}\frac{r_i^2}{\nu} \tag{2}$$

is the droplet response (or Stokes) time attributed to the superdroplet, $\nu = 10^{-5}\,\mathrm{m^2\,s^{-1}}$ is the viscosity of air, and ρ is the mass density of the airflow.

Droplet collisions are represented by collisions of superdroplets (Shima et al. 2009; Johansen et al. 2012; Li et al. 2017), as mentioned above. Superdroplets i and j residing inside a grid cell collide with probability

$$p_{ij} = \lambda_{ij}\delta t\,, \tag{3}$$

where δt is the integration time step. A collision happens when $\eta < p_{ij}$, where $0 \leq \eta \leq 1$ is a uniformly distributed random number. To avoid a probability larger than unity, we limit the integration step through the condition $\delta t < 1/\lambda_{ij}$. The collision rate is

$$\lambda_{ij} = \pi \left(r_i + r_j\right)^2 |\boldsymbol{v}_i - \boldsymbol{v}_j| \, E_{ij} \, \frac{\xi_{\max}}{\delta x^3}, \tag{4}$$

where E_{ij} is the collision efficiency, $\xi_{\max} = \max(\xi_i, \xi_j)$ is the larger one of the two ξ values for superdroplets i or j (Table 1), and δx^3 is the volume of the grid cell closest to the superdroplet. Note that equation (4) implies that background droplets, which all have the same radius (and therefore $\boldsymbol{v}_i = \boldsymbol{v}_j$, so $\lambda_{ij} = 0$) can never collide among themselves. Moreover, no collisions are possible between physical particles within a single superdroplet, because their velocity difference vanishes. To facilitate the comparison with the earlier work, we assume $E_{ij} = 1$ for most of our simulations. To assess the effects of this assumption, we also compare with results where the efficiency increases with droplet radius (Lamb and Verlinde 2011). Following Kostinski and Shaw (2005) and Wilkinson (2016), we adopt a simple power law prescription for the dependence of the efficiency on the droplet radius.

What happens when two superdroplets collide? To write down the rules, we denote the number of droplets in superdroplet i by ξ_i, while ξ_j is the number of droplets in superdroplet j. M_i and M_j are the corresponding droplet masses. The collision scheme suggested by Shima et al. (2009) amounts to the following rules; see also Figure 1 for an illustration. To ensure mass conservation between superdroplets i and j, when $\xi_j > \xi_i$, which is the case illustrated in Figure 1(b), droplet numbers and masses are updated such that

$$\begin{aligned} \xi_i &\to \xi_i, \quad \xi_j \to \xi_j - \xi_i, \\ M_i &\to M_i + M_j, \quad M_j \to M_j. \end{aligned} \tag{5}$$

When $\xi_j < \xi_i$, which is the case shown in Figure 1(a), the update rule is also given by equation (5), but with indices i and j exchanged. In other words, the number of droplets in the smaller superdroplet remains unchanged (and their masses are increased), while that in the larger one is reduced by the amount of droplets that have collided with all the droplets of the smaller superdroplet (and their masses remain unchanged).

To ensure momentum conservation during the collision, the momenta of droplets in the two superdroplets are updated as

$$\begin{aligned} \boldsymbol{v}_i M_i &\to \boldsymbol{v}_i M_i + \boldsymbol{v}_j M_j \,, \\ \boldsymbol{v}_j M_j &\to \boldsymbol{v}_j M_j \,, \end{aligned} \tag{6}$$

after a collision of superdroplets.

Finally, when $\xi_i = \xi_j$, which is the case described in Figure 1(c), droplet numbers and masses are updated as

$$\begin{aligned} &\xi_i \to \xi_i/2 \,, \quad \xi_j \to \xi_j/2 \,, \\ &M_i \to M_i + M_j \,, \quad M_j \to M_i + M_j \,. \end{aligned} \tag{7}$$

It is then assumed that, when two superdroplets, each with less than one physical droplet, collide, the superdroplet containing the smaller physical droplet is collected by the more massive one; it is thus removed from the computational domain after the collision. We emphasize that equation (5) does not require ξ to be an integer. Since we usually specify the initial number density of physical particles, ξ can be fractional from the beginning. This is different from the integer treatment of ξ in Shima et al. (2009).

The superdroplet simulations are performed by using the particle modules of the Pencil Code (Pencil Code Collaboration et al. 2021). The fluid dynamics modules of the code are not utilized here. To reduce the computational cost and make it linear in the number of superdroplets per mesh point, $n_{\rm s}(t)$, Shima et al. (2009) supposed that each droplet interacts at most with one other one, which is what Shima et al. (2009) refer to as random permutation technique or linear sampling technique. This technique was also adopted by Dziekan and Pawlowska (2017), and also by Unterstrasser et al. (2020). It is not used in the Pencil Code, because it could reduce the statistical accuracy of the results. Furthermore, it is important to emphasize that the computational cost is in either case only linear in the *total* number of superdroplets, because we do not allow for collisions between superdroplets that are not in the proximity of the same mesh point. In the Pencil Code, collisions between particles residing within a given grid cell are evaluated by the same processor which is also evaluating the fluid equations of that grid cell. Due to this, together with the domain

decomposition used in the code, the particle collisions are automatically efficiently parallelized as long as the particles are more or less uniformly distributed over the domain. For the purpose of the present study, we designed a parallel technique to run thousands of one-dimensional (1-D) superdroplet simulations simultaneously.

b. Numerical setup

In our superdroplet simulations, we consider droplets of radius $10\,\mu$m, randomly distributed in space, together with one droplet of twice the mass and radius $2^{1/3} \times 10\,\mu\text{m} = 12.6\,\mu\text{m}$. The larger droplet has a higher settling speed than the $10\,\mu$m droplets and sweeps them up through collision and coalescence. For each simulation, we track the growth history of the larger droplet until it reaches $50\,\mu$m in radius and record the time T it takes to grow to that size.

In the superdroplet algorithm, one usually takes $\xi_i(t_0) \gg 1$, which implies that the actual number of lucky droplets is also more than one. This was not intended in the original formulation of the lucky droplet model (Telford 1955; Kostinski and Shaw 2005; Wilkinson 2016) and could allow the number of superdroplets with heavier (lucky) droplets, $N_{\text{s}}^{(\text{luck})}$, to become larger than unity. This would manifest itself in the growth history of the lucky droplets through an increase by more than the mass of a background droplet. We refer to this as "jumps". Let us therefore now discuss the conditions under which this would happen and denote the values of $\xi(t_0)$ for the lucky and background droplets by ξ_{luck} and ξ_{back}, respectively. First, for $\xi_{\text{luck}} = \xi_{\text{back}}$, the masses of both lucky and background superdroplets can increase, provided their values of $\xi(t_0)$ are above unity; see Figure 1(c). Second, even if $\xi_{\text{luck}} < \xi_{\text{back}}$ initially, new lucky superdroplets could in principle emerge when the *same* two superdroplets collide with each other multiple times. This can happen for two reasons. First, the use of periodic boundary conditions for the superdroplets (i.e., in the vertical direction in our laminar model with gravity). Second, two superdroplets can remain at the same location (corresponding to the same mesh point of the Eulerian grid for the fluid) during subsequent time steps. The simulation time step must be less than both the time for a superdroplet to cross one grid spacing and the mean collision time, i.e., the inverse collision rate given by equation (4). Looking at Figure 1, we see that ξ_{back} can then decrease after each collision and potentially become equal to or drop below the value of ξ_{luck}. This becomes exceedingly unlikely if initially $\xi_{\text{back}} \gg \xi_{\text{luck}}$, but it is not completely impossible, unless ξ_{luck} is chosen initially to be unity.

The initial value of $\xi_{\rm back}$ can in principle also be chosen to be unity. Although such a case will indeed be considered here, it would defeat the purpose and computational advantage of the superdroplet algorithm. Therefore, we also consider the case $\xi_{\rm back} \gg \xi_{\rm luck}$. As already mentioned, jumps are impossible if $\xi_{\rm luck}$ is unity. For orientation, we note that the speed of the lucky droplet prior to the first collision is about $3.5\,{\rm cm\,s^{-1}}$, the average time to the first collision is 490 s, and thus, it falls over a distance of about 17 m before it collides.

The superdroplet algorithm is usually applied to 3-D simulations. If there is no horizontal mixing, one can consider 1-D simulations. Moreover, we are only interested in the column in which the lucky droplet resides. In 3-D, however, the number density of the $10\,\mu$m droplets beneath the lucky one is in general not the same as the mean number density of the whole domain. This leads to yet another element of randomness that we shall consider in this paper by studying the difference between 1-D and 3-D simulations, and fluctuations of the number density between columns.

Equation (1) is solved with periodic boundary conditions using the Pencil Code (Pencil Code Collaboration et al. 2021), which employs a third-order Runge-Kutta time stepping scheme. The superdroplet algorithm is implemented in the Pencil Code, which is used to solve equation (3)–equation (7). We perform 1-D simulations to mimic the settling of cloud droplets purely due to gravity. 3-D simulations are conducted to investigate how the spatial distribution of cloud droplets affects the collision process. For the 1-D superdroplet simulations, we employ an initial number density of background droplets of $n_0 \approx 3\times10^8\,{\rm m^{-3}}$ within a volume $V = L_x \times L_y \times L_z$ with $L_x = L_y = 0.002\,{\rm m}$, $L_z = 0.214\,{\rm m}$, and $N_{\rm s}(t_0) = 256$ such that the multiplicity is $\xi_{\rm luck}(t_0) = \xi_{\rm back}(t_0) = 1$. For each simulation, 7,686,000 time steps are integrated with an adaptive time step with a mean value of $\delta t = 2.942\times10^{-4}\,{\rm s}$. For 3-D simulations, we use $n_0 = 3\times10^8\,{\rm m^{-3}}$, $V = 8.847\times10^{-7}\,{\rm m^3}$ ($L_x = L_y = L_z = 0.0096\,{\rm m}$), and $N_{\rm s}(t_0) = 128$ with multiplicity $\xi_{\rm luck}(t_0) = \xi_{\rm back}(t_0) = 2$. There are about 10^7 time steps integrated with a time step $\delta t = 1.04\times10^{-4}\,{\rm s}$. We use a cubic mesh with $N_{\rm grid} = 4^3$ points and perform 1000 simulations for both cases. For a superdroplet with an initial radius $12.6\,\mu$m to grow to $50\,\mu$m, 123 collisions are required.

3. Lucky-droplet models

a. Basic idea

In its simplest form, the LDM describes the collisional growth of a larger droplet that settles through a quiescent fluid and collides with smaller monodisperse droplets, that were initially randomly distributed in space. This corresponds to the setup described in the previous section. We begin by recalling the main conclusions of Kostinski and Shaw (2005). Initially, the lucky droplet has a radius corresponding to a volume twice that of the background droplets, whose radius was assumed to be $r_1 = 10\,\mu$m. Therefore, its initial radius is $r_2 = 2^{1/3} r_1 = 12.6\,\mu$m. After the $(k-1)$th collision step with smaller droplets, it increases as

$$r_k \sim r_1 k^{1/3}. \tag{8}$$

Fluctuations in the length of the time intervals t_k between collision $k-1$ and k give rise to fluctuating growth histories of the larger droplet. These fluctuations are quantified by the distribution of the cumulative time

$$T = \sum_{k=2}^{124} t_k, \tag{9}$$

corresponding to 123 collisions needed for the lucky droplet to grow from $12.6\,\mu$m to $50.0\,\mu$m. [Note that Kostinski and Shaw (2005) used one more collision, so their final radius was actually $50.1\,\mu$m.] The time intervals t_k between successive collisions are drawn from an exponential distribution with a probability $p_k(t_k) = \lambda_k \exp(-\lambda_k t_k)$. The rates λ_k depend on the differential settling velocity $|\boldsymbol{v}_k - \boldsymbol{v}_1|$ between the colliding droplets through equations (3) and (4). Here, however, the background droplets have always the radius r_1, so the collision rate at the $(k-1)$th collision of the lucky droplet with radius r_k obeys

$$\lambda_k = \pi\,(r_k + r_1)^2\,|\boldsymbol{v}_k - \boldsymbol{v}_1|\,E_k\,n^{\mathrm{back}}, \tag{10}$$

where $E_k = E(r_k, r_1)$, and $\boldsymbol{v}_k$ and $\boldsymbol{v}_1$ are approximated by their terminal velocities.

While the LDM is well suited for addressing theoretical questions regarding the significance of rare events, it should be emphasized that it is at the same time highly idealized. Furthermore,

while it is well known that $E_k \ll 1$ (Pruppacher and Klett 1997), it is instructive to assume, as an idealization, $E_k = 1$ for all k, so the collision rate (10) can be approximated as $\lambda_k \sim r_k^4$ (Kostinski and Shaw 2005), which is permissible when $r_k \gg r_1$. It follows that, in terms of the collision index k, the collision frequency is

$$\lambda_k = \lambda_* k^{4/3}, \tag{11}$$

where $\lambda_* = (2\pi/9)(\rho_\mathrm{d}/\rho)(gn/\nu)r_1^4$, and n is the number density of the $10\,\mu$m background droplets. This is essentially the model of Kostinski and Shaw (2005) and Wilkinson (2016), except that they also assumed $E_k \neq 1$. They pointed out that, early on, i.e., for small k, λ_k is small and therefore the mean collision time λ_k^{-1} is long. We note that the variance of the mean collision time is λ_k^{-2}, which is large for small k. The actual time until the first collision can be very long, but it can also be very short, depending on fluctuations. Therefore, at early times, fluctuations have a large impact on the cumulative collision time. Note that for droplets with $r \geq 30\,\mu$m, the linear Stokes drag is not valid (Pruppacher and Klett 1997).

b. Relaxing the power law approximation

We now discuss the significance of the various approximations being employed in the mathematical formulation of the LDM of Kostinski and Shaw (2005). To relax the approximations made in equation (11), we now write it in the form

$$\lambda_k = \lambda_* E_k r_\mathrm{A}^2(r_k) r_\mathrm{B}^2(r_k)/r_1^4 \quad (k \geq 2), \tag{12}$$

where

$$r_\mathrm{A}^2 = (r_k + r_1)^2, \quad r_\mathrm{B}^2 = r_k^2 - r_1^2 \tag{13}$$

would correspond to the expression equation (10) used in the superdroplet algorithm. In equation (11), however, it was assumed that $r_\mathrm{A} = r_\mathrm{B} = r_k$. To distinguish this approximation from the form used in equation (12), we denote that case by writing symbolically "$r_\mathrm{A} \neq r_k \neq r_\mathrm{B}$"; see Figure 2.

In equation (13), we have introduced r_A and r_B to study the effect of relaxing the assumption $r_\mathrm{A} = r_\mathrm{B} = r_k$, made in simplifying implementations of the LDM. Both of these assumptions are

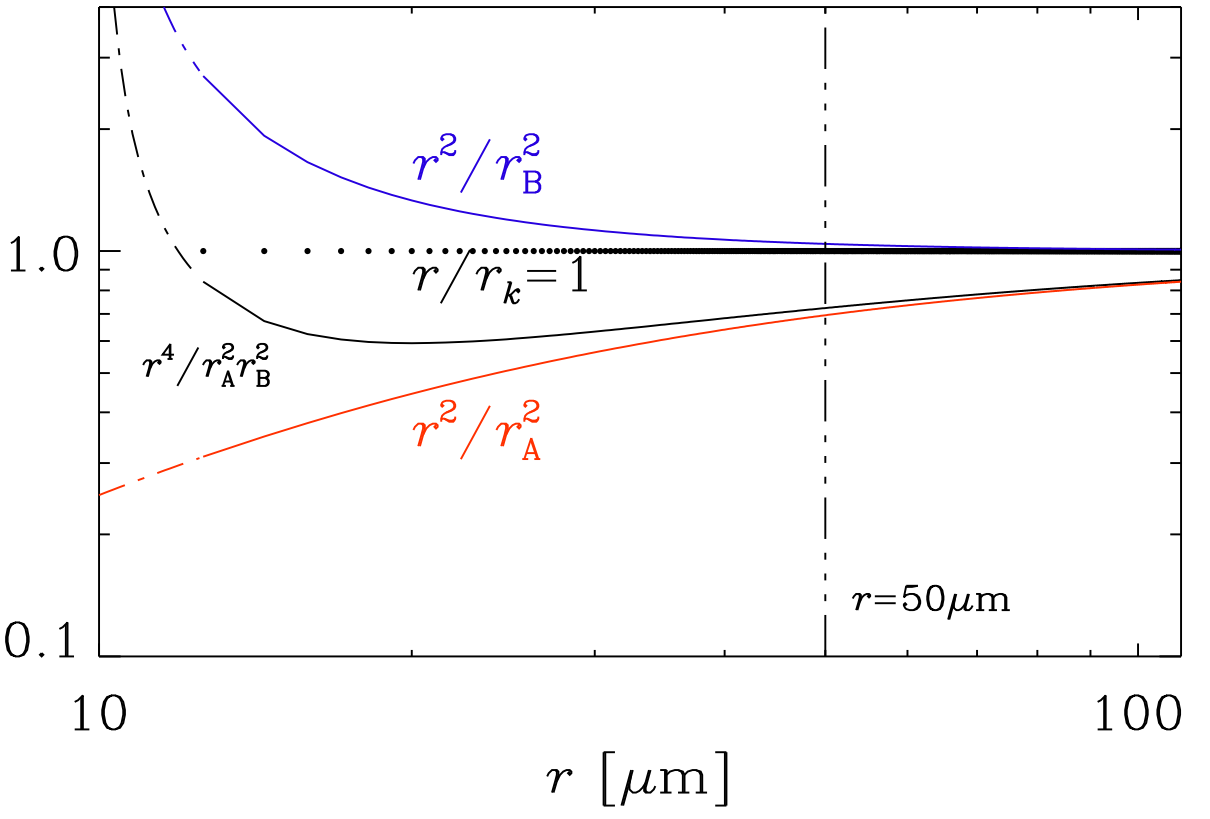

FIG. 2. Contributions to the two correction factors r^2/r_A^2 (red) and r^2/r_B^2 (blue), as well as their product. The discrete radii r_k for $k \geq 2$ are shown in a horizontal line of dots. The vertical dash-triple-dotted lines denote the radius $r = 50\,\mu$m.

justified at late times when the lucky droplet has become large compared to the smaller ones, but not early on, when the size difference is moderate.

By comparison, in mean-field theory (MFT), one assumes deterministic collision times that are given by $t_k = \lambda_k^{-1}$. In Figure 3 we demonstrate the effect of the contributions from r_A and r_B on the mean cumulative collision time in the corresponding MFT,

$$T_k^{\mathrm{MFT}} = \sum_{k'=2}^{k} t_{k'}^{\mathrm{MFT}}, \tag{14}$$

where

$$t_k^{\mathrm{MFT}} = \lambda_k^{-1} \tag{15}$$

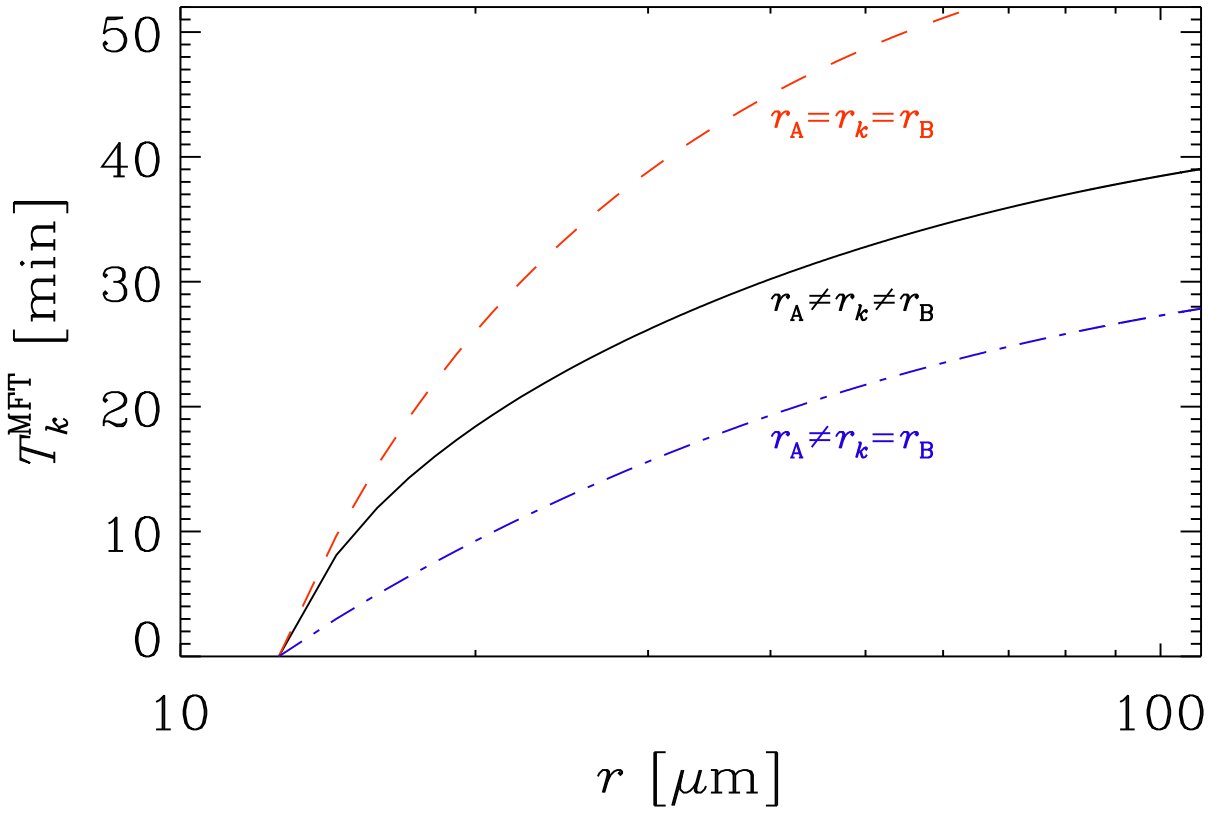

FIG. 3. Cumulative mean collision times, $T_k^{\rm MFT}$, for $r_{\rm A} \neq r_k \neq r_{\rm B}$ (solid black line), compared with the approximations $r_{\rm A} = r_{\rm B} = r_k$ (red dashed line) and only $r_{\rm B} = r_k$ (blue dash-dotted line).

are the inverse of the mean collision rates. We see that, while the contribution from $r_{\rm A}$ shortens the mean collision time, that of $r_{\rm B}$ enhances it. In Figure 2, we also see that the contributions to the two correction factors $r^2/r_{\rm A}^2$ and $r^2/r_{\rm B}^2$ have opposite trends, which leads to partial cancelation in their product.

In Figure 4 we show a comparison of the distribution of cumulative collision times for various representations of r_k using approach I. Those are computed numerically using 10^{10} realizations of sequences of random collision times t_k. To perform this many realizations, we use the `special/lucky_droplet` module of the PENCIL CODE (Pencil Code Collaboration et al. 2021); see Appendix A1 for details.

The physically correct model is where $r_{\rm A} \neq r_k \neq r_{\rm B}$ (black line in Figure 4). To demonstrate the sensitivity of $P(T)$ to changes in the representation of r_k, we show the result for the approximations

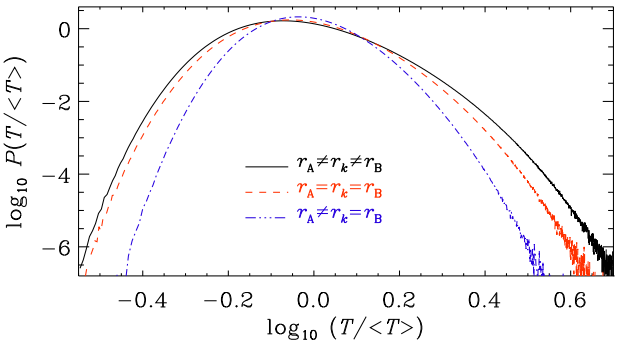

FIG. 4. Comparison of $P(T)$ in a double-logarithmic representation for the LDM appropriate to our benchmark (black solid line) with various approximations where $r_A = r_B = r_k$ (red dashed line) along with a case where only $r_B = r_k$ is assumed (blue dash-dotted line). Here we used approach I with 10^{10} realizations.

$r_A = r_k = r_B$ (red line) and $r_A \neq r_k = r_B$ (blue line). The $P(T)$ curve is also sensitive to changes in the collision efficiency late in the evolution. To demonstrate this, we assume $E_k \propto r_k^2$ when $r_k \geq r_*$ (Lamb and Verlinde 2011). To ensure that $E_k \leq 1$, we take

$$E_k = E_* \max\left(1, (r/r_*)^2\right), \tag{16}$$

with $E_* = (r_*/50\,\mu\text{m})^2$. However, the normalized $P(T)$ curves are independent of the choice of the value of E_*. In Figure 5, we show the results for $r_A \neq r_k \neq r_B$ using $r_* = 40\,\mu$m and $30\,\mu$m (red and blue lines, respectively) and compare with the case $E_k = \text{const}$. The more extreme cases with $r_* = 20\,\mu$m and $10\,\mu$m are shown as gray lines. The latter is similar to the case $\lambda_k \sim r_k^6$ considered by Kostinski and Shaw (2005) and Wilkinson (2016).

When $r_A = r_k = r_B$, or only $r_k = r_B$, the $P(T)$ curves exhibit smaller widths. By contrast, when the collision efficiency becomes quadratic later on (when $r > r_* \equiv 30\,\mu$m or $40\,\mu$m), the $P(T)$ curves have larger widths; see Figure 5. To quantify the shape of $P(T)$, we give in Table 2 the average of $X \equiv \ln(T/\langle T\rangle)$, its standard deviation $\sigma = \langle x^2\rangle^{1/2}$, where $x \equiv X - \langle X\rangle$, its skewness skew $X = \langle x^3\rangle/\sigma^3$, and its kurtosis kurt $X = \langle x^4\rangle/\sigma^4 - 3$. We recall that, for a perfectly lognormal distribution, skew $X =$ kurt $X = 0$. The largest departure from zero is seen in the skewness, which is positive, indicating that the distribution is somewhat enhanced for long times. The kurtosis is rather small, however.

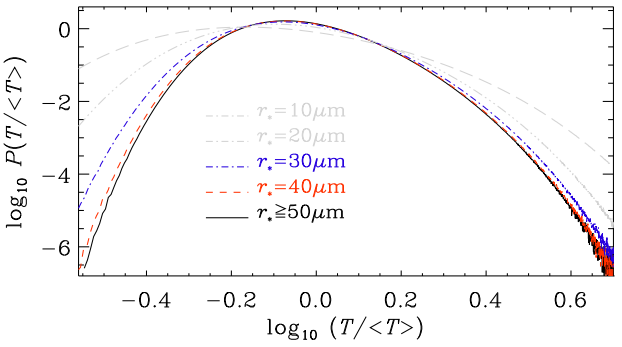

FIG. 5. Comparison of $P(T)$ in a double-logarithmic representation for the LDM for $r_* = 40\,\mu$m and $30\,\mu$m using $r_A \neq r_k \neq r_B$. The black line agrees with that in Figure 4, and the two gray lines refer to the cases with $r_* = 20\,\mu$m and $10\,\mu$m. Here we used approach I with 10^{10} realizations.

TABLE 2. Moments of $X = \ln(T/\langle T\rangle)$ computed from 10^{10} realizations for different values of r_* (in μm), and different prescriptions of r_A and r_B. The corresponding values of T_{124}^{MFT} are also given and are normalized to unity for $r_A \neq r_k \neq r_B$ with $r_* \geq 50\,\mu$m.

r_*	r_A	r_B	T_{124}^{MFT}	$\langle X\rangle$	$\sigma(X)$	skew X	kurt X
—	—	r_k	0.67	−0.020	0.21	0.22	0.08
—	r_k	r_k	1.49	−0.033	0.25	0.25	0.05
—	—	—	1	−0.040	0.28	0.34	0.10
40	—	—	0.99	−0.041	0.28	0.33	0.09
30	—	—	0.93	−0.046	0.30	0.28	0.05
20	—	—	0.79	−0.063	0.35	0.18	−0.04
10	—	—	0.34	−0.111	0.47	0.16	−0.17

The main conclusion that can be drawn form the investigation mentioned above is that, as far as the shapes of the different curves is concerned, it does not result in any significant error to assume $r_k \gg r_1$. The value of σ is only about 10% smaller if $r_A = r_k = r_B$ is used (compare the red dashed and black solid lines in Figure 4). This is because the two inaccuracies introduced by r_A and r_B almost cancel each other. When $r_* = 40\,\mu$m or $30\,\mu$m, for example, the values of σ increase by 3% and 15%, respectively; see Table 3, where we also list the corresponding values of T_{124}^{MFT}. On the other hand, the actual averages such as $\langle T\rangle \approx T_{124}^{MFT}$ vary by almost 50%.

Here and below, we plot the distribution of the cumulative times versus the normalized time, $T/\langle T\rangle$, as was done in the work of Kostinski and Shaw (2005). Normalizing by $\langle T\rangle$ allows us to see changes in the shape of $P(T/\langle T\rangle)$, thus allows a more direct comparison of the subtle differences

in the shapes of the different curves and ensures that the peaks of all curves are at approximately the same position. We normally compute $\langle T \rangle$ as an average over all realizations, but these averages also agree with T_{124}^{MFT}.

A straightforward extension of the LDM is to take horizontal variations in the local column density into account. Those are always present for any random initial conditions, but could be larger for turbulent systems, regardless of the droplet speeds. Indeed, in our 3-D superdroplet simulations, large droplets can fall in different vertical columns that contain different numbers of small droplets, a consequence of the fact that the small droplets are initially randomly distributed. To describe the results of our 3-D simulations, it is necessary to solve for an ensemble of columns with different number density of the $10\,\mu$m background droplets and compute the distribution of cumulative collision times. We present a corresponding comparison with our superdroplet algorithm at the end of this paper.

c. Relation to the superdroplet algorithm

To understand the nature of the superdroplet algorithm, and why it captures the lucky droplet problem accurately, it is important to realize that the superdroplet algorithm is actually a combination of two separate approaches, each of which turns out to be able to reproduce the lucky droplet problem to high precision. In principle, we can distinguish four different approaches to obtaining the collision time interval t_k. In approach I, t_k was taken from an exponential distribution of random numbers. Another approach is to use a randomly distributed set of $10\,\mu$m background droplets and then to solve for the collisions between the lucky droplets and the background explicitly (approach II). A third approach is to use a Monte Carlo method to solve for the time evolution to decide whether at any time there is a collision or not (approach III). This is actually what is done within each grid cell in the superdroplet algorithm; see equations (3) and (4). The fourth approach is the superdroplet algorithm discussed extensively in section 2.a (approach IV). It is essentially a combination of approaches II and III. We have compared all four approaches and found that they all give very similar results. In the following, we describe approaches II and III in more detail, before focussing on approach IV in section 4.

TABLE 3. Summary of the four approaches.

Approach	Description
I	time interval t_k drawn from distribution
II	true Lagrangian particles collide
III	probabilistic, just a pair of superdroplets
IV	superdroplet model (combination of II & III)

d. Solving for the collisions explicitly

A more realistic method (approach II) is to compute random realizations of droplet positions in a tall box of size $L_\mathrm{h}^2 \times L_z$, where L_h and L_z are the horizontal and vertical extents, respectively. We position the lucky droplet in the middle of the top plane of the box. Collisions are only possible within a vertical cylinder of radius $r_k + r_1$ below the lucky droplet. Next, we calculate the distance Δz to the first collision partner within the cylinder. We assume that both droplets reach their terminal velocity well before the collision. This is an excellent approximation for dilute systems such as clouds, because the droplet response time τ_k of equation (2) is much shorter than the mean collision time. Here we use the subscript k to represent the time until the $(k-1)$th collision, which is equivalent to the ith droplet. We can then assume the relative velocity between the two as given by the difference of their terminal velocities as

$$\Delta v_k = (\tau_k - \tau_1)\, g. \tag{17}$$

The time until the first collision is then given by $t_2 = \Delta z / \Delta v_2$. This collision results in the lucky droplet having increased its volume by that of the $10\,\mu$m droplet. Correspondingly, the radius of the vertical cylinder of collision partners is also increased. We then search for the next collision partner beneath the position of the first collision, using still the original realization of $10\,\mu$m droplets. We continue this procedure until the lucky droplet reaches a radius of $50\,\mu$m.

e. The Monte Carlo method to compute t_k

In the Monte Carlo method (approach III) we choose a time step δt and step forward in time. As in the superdroplet algorithm, the probability of a collision is given by $p_k = \lambda_k \delta t$; see equation (3). We continue until a radius of $50\,\mu$m is reached. We note that in this approach, n is kept constant, i.e., no background droplet is being removed after a collision.

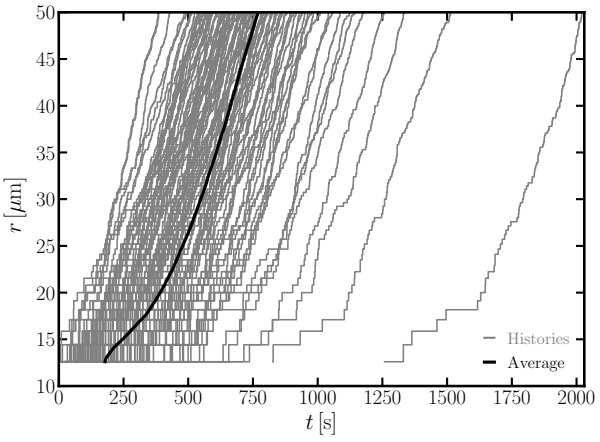

FIG. 6. 98 growth histories of lucky droplets obtained from 98 independent 1-D superdroplet simulations (approach IV), as described in the text. All superdroplets have initially the same number of droplets, $\xi_i(t_0) = 1$ with $N_s(t_0) = 256$. The mean number density of droplets is $n_0 = 3 \times 10^8\,\mathrm{m}^{-3}$. The fat solid line shows the average time for each radius.

Approach III also allows us to study the effects of jumps in the droplet size by allowing for several lucky droplets at the same time and specifying their collision probability appropriately. These will then be able to interact not only with the $10\,\mu$m background droplets, but they can also collide among themselves, which causes the jumps. We will include this effect in solutions of the LDM using approach III and compare with the results of the superdroplet algorithm.

4. Results

a. Accuracy of the superdroplet algorithm

We now want to determine to what extent the fluctuations are correctly represented by the superdroplet algorithm. For this purpose, we now demonstrate the degree of quantitative agreement between approaches I–III and the corresponding solution with the superdroplet algorithm (approach IV). This is done by tracking the growth history of each lucky droplet. As the first few collisions determine the course of the formation of larger droplets, we also use the distribution $P(T)$ of cumulative collision times T. We perform N_{real} superdroplet simulations with different random seeds using $\xi_i(t_0) = 1$.

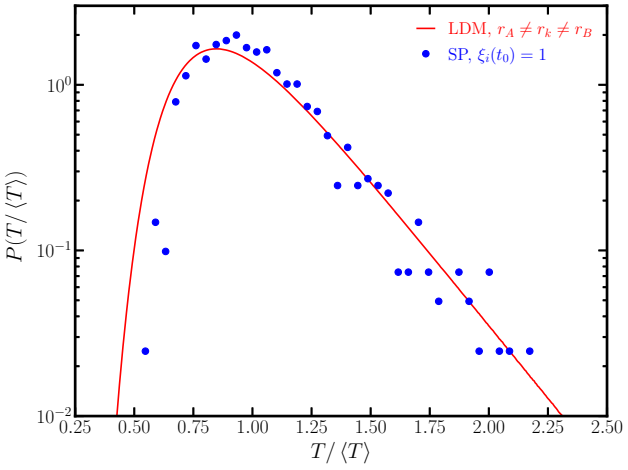

FIG. 7. Corresponding $P(T)$ of Figure 6 obtained with the superdroplet algorithm (blue dots) and the LDM using approach I with $r_A \neq r_k \neq r_B$ (red solid line).

We begin by looking at growth histories for many individual realizations obtained from the superdroplet simulation. Figure 6 shows an ensemble of growth histories (thin gray lines) obtained from $N_{\text{real}} \approx 10^3$ independent simulations, as described above. The times between collisions are random, leading to a distribution of cumulative growth times to reach $50\,\mu$m. Also shown is the mean growth curve (thick black line), obtained by averaging the time at fixed radii r. This figure demonstrates that the fluctuations are substantial. We also see that large fluctuations relative to the average time are rare.

To quantify the effect of fluctuations from all realizations, we now consider the corresponding $P(T)$ in Figure 7. We recall that $\xi_i(t_0) = 1$ for our superdroplet simulation in Figure 7. However, a simulation with $\xi_i(t_0) = 50$ yields almost the same result; see Appendix A2.

The comparison of the results for the LDM using approach I and the superdroplet algorithm shows small differences. The width of the $P(T)$ curve is slightly larger for approach I than for the superdroplet simulations. This suggests that the fluctuations, which are at the heart of the LDM, are slightly underrepresented in the superdroplet algorithm.

An important question is to what extent our results depend on the density of background droplets and the size of the computational domain. To examine this with the superdroplet algorithm (approach IV), we consider three values of the initial number density: $n_0 = 3 \times 10^8\,\text{m}^{-3}$, $10n_0$, and $100n_0$. Figure 8 shows $P(T)$ for these three cases using first the cumulative time T [Figure 8(a)]

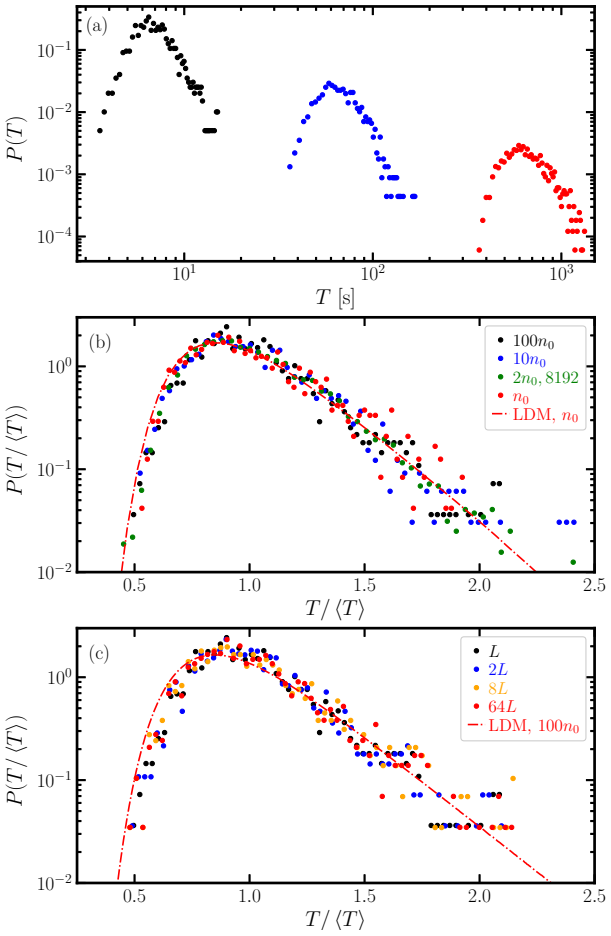

FIG. 8. (a): $P(T)$ for n_0 (red), $10n_0$ (blue), and $100n_0$ (black) with $n_0 = 3\times10^8\,\mathrm{m}^{-3}$ and $L = 0.214\,\mathrm{m}$ and (b): $P(T/\langle T\rangle)$ n_0, $2n_0$ (green), $10n_0$, and $100n_0$ and (c): $P(T/\langle T\rangle)$ for L, $2L$, $8L$, and $64L$ with $100n_0$, obtained using the superdroplet algorithm (approach IV). The red dash-dotted line in (b) represents the LDM (approach I) with $r_\mathrm{A} \neq r_k \neq r_\mathrm{B}$ and $n_0 = 3\times10^8\,\mathrm{m}^{-3}$, which is the same simulation as the one in Figure 7. The green line in (b) is for 8192 realizations, while all the other simulations are for 1024 realizations.

and then the normalized time $T/\langle T\rangle$ [Figure 8(b)]. We see that the positions of the peaks in $P(T)$ change linearly with the initial number density n_0, but $P(T/\langle T\rangle)$ are very similar to each other. This is related to the fact that, after normalization, n_0 drops out from the expression for $t_k/\langle T\rangle$ in the LDM (approach I); see equation (9). At small values of $T/\langle T\rangle$, however, all curves show a similar slight underrepresentation of the fluctuations as already seen in Figure 7. In all these simulations, we used 1024 realizations, except for one case where we used 8192 realizations; see the green line

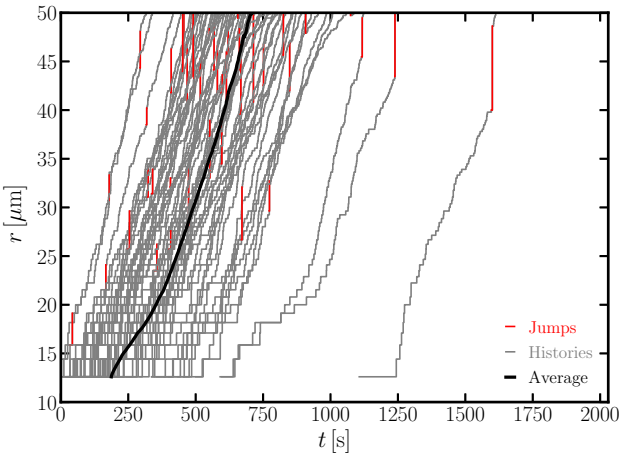

FIG. 9. Same as Figure 6 but with initial condition $\xi_i(t_0) = 2$ using $N_s(t_0) = 128$. Note the occurrence of jumps, indicated in red.

in Figure 8(b). The distribution of cumulative growth times is obviously much smoother in the latter case, but the overall shape is rather similar.

In our superdroplet simulations (approach IV), the vertical extent of the simulation domain is only $L = 0.214\,\mathrm{m}$. This is permissible given that we use periodic boundary conditions for the particles, and that the number of particles is approximately constant. Nevertheless, the accuracy of our results may suffer from poor statistics. To investigate this in more detail, we now perform 1-D simulations with $2L$, $8L$, and $64L$. At the same time, we increased the number of mesh points and the number of superdroplets by the same factors. Since the shape of $P(T/\bar{T})$ is almost independent of n_0, as shown in Figure 8(b), we use $n_0 = 3\times10^{10}\,\mathrm{m}^{-3}$ instead of $n_0 = 3\times10^{8}\,\mathrm{m}^{-3}$ to save computational power. As shown in Figure 8(c), $P(T/\bar{T})$ is insensitive to the domain size. Therefore, our results with $L = 0.214\,\mathrm{m}$ can be considered as accurate with respect to $P(T/\bar{T})$.

In the following, we discuss how our conclusions relate to those of earlier work. We then discuss a number of additional factors that can modify the results (jumps in r or the effects of 3-D, for example). Those additional factors can also be taken into account in the LDM. Even in those cases, it turns out that the differences between the LDM and the superdroplet algorithm are small.

b. The occurrence of jumps

One of the pronounced features in our superdroplet simulations with $\xi_i(t_0) > 1$ is the possibility of jumps. We see examples in Figure 9 where $\xi_{\rm luck} = \xi_{\rm back} = 2$ and the jumps are visualized by the red vertical lines. Those jumps are caused by the coagulation of the lucky droplet with droplets of radii larger than $10\,\mu$m that were the result of other lucky droplets in the simulations. What is the effect of these jumps? Could they be responsible for the behavior found by Dziekan and Pawlowska (2017) that the difference in their $t_{10\%}$ between the numerical and theoretical calculation decreases with the square root of the number of physical droplets, as discussed in section 1?

It is clear that those jumps occur only at late times when there has been enough time to grow several more lucky droplets. Because the collision times are so short at late times, the jumps are expected to be almost insignificant. To quantify this, it is convenient to use approach III, where we choose $N_{\rm s}^{\rm (luck)} = 3$ superdroplets simultaneously. (As always in approach III, the background particles are still represented by only one superdroplet, and n is kept constant.) We also choose $\xi_{\rm luck} = 1$, and therefore $N_{\rm d}^{\rm (luck)} = 3$. The lucky droplets can grow through collisions with the $10\,\mu$m background droplets and through mutual collisions between lucky droplets. The collision rate between lucky droplets i and j is, analogously to equation (12), given by

$$\lambda_{ij}^{\rm (luck)} = \pi \left(r_i + r_j\right)^2 |\boldsymbol{v}_i - \boldsymbol{v}_j|\, n_{\rm luck}, \tag{18}$$

where $n_{\rm luck}$ is the number density of physical droplets in the superdroplet representing the lucky droplet. To obtain an expression for $n_{\rm luck}$ in terms of the volume of a grid cell δx^3, we write $n_{\rm luck} = \xi_{\rm luck}/\delta x^3$. The ratio of the physical number of lucky droplets, $N_{\rm d}^{\rm (luck)}$, to the physical number of background droplets, $N_{\rm d}^{\rm (back)}$ is given by

$$\epsilon = \frac{N_{\rm d}^{\rm (luck)}}{N_{\rm d}^{\rm (back)}} = \frac{\xi_{\rm luck}\, N_{\rm s}^{\rm (luck)}}{\xi_{\rm back}\, N_{\rm s}^{\rm (back)}}. \tag{19}$$

To investigate the effect of jumps on $P(T)$ in the full superdroplet model studied above (see Figures 6 and 9), we first consider the case depicted in Figure 6, where $\xi_{\rm luck} = \xi_{\rm back} \equiv \xi_i(t_0) = 1$. Here, we used $N_{\rm s} = 256$ superdroplets, of which one contained the lucky droplet, so $N_{\rm s}^{\rm (luck)} = 1$, and the other 255 superdroplets contained a $10\,\mu$m background droplet each. In our superdroplet

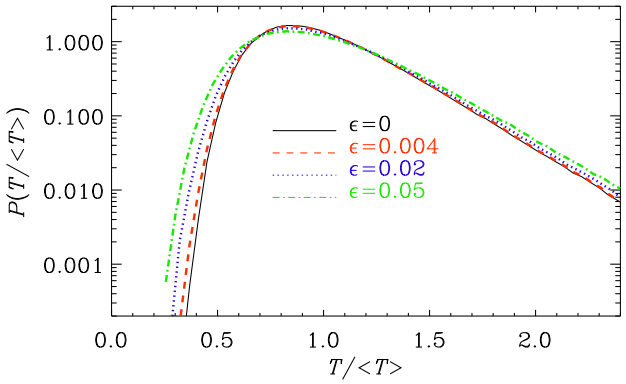

FIG. 10. Comparison of models with $\epsilon = 0$ (no jumps), 0.004 (the value expected for the simulations), 0.02, and 0.05 using approach III.

solution, the ratio (19) was therefore $\epsilon = 1/255 = 0.004$. Using approach III, ϵ enters simply as an extra factor in the collision probability between different lucky droplets. (In approach III, all quantities in equation (19) are kept constant.) The effect on $P(T)$ is shown in Figure 10, where we present the cumulative collision times for models with three values of ϵ using approach III. We see that for small values of ϵ, the cumulative distribution function is independent of ϵ, and the effect of jumps is therefore negligible (compare the black solid and the red dashed lines of Figure 10). More significant departures due to jumps can be seen when $\epsilon = 0.02$ and larger.

Let us now compare with the case in which we found jumps using the full superdroplet approach (approach IV). The jumps in the growth histories cause the droplets to grow faster than without jumps. However, jumps do not have a noticeable effect upon $P(T)$ in the superdroplet simulations we conducted; see Figure 11. By comparing $P(T)$ for $\xi_{\rm back} = 40$ (blue crosses in Figure 11) with that for $\xi_{\rm back} = 2$ (black circles), while keeping $\xi_{\rm luck} = 2$ in both cases, hardly any jumps occur and the lucky droplet result remains equally accurate.

For larger values of ϵ, jumps occur much earlier, as can be seen from Figure 12, where we show 30 growth curves for the cases $\epsilon = 0.004$, which is relevant to the simulations of Figure 7, as well as $\epsilon = 0.02$, and 0.05. We also see that for large values of ϵ, the width in the distribution of arrival times is broader and that both shorter and longer times are possible. This suggests that the reason for the finite residual error in the values of $t_{10\%}$ found by Dziekan and Pawlowska (2017) for $\xi_i(t_0) > 9$ could indeed be due to jumps. In our superdroplet simulations, by contrast, jumps cannot occur when $\xi_i(t_0) = 1$ or $\xi_{\rm back} \gg \xi_{\rm luck}$.

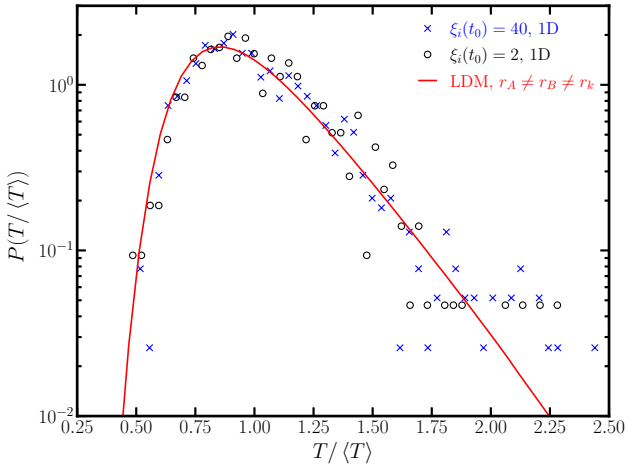

FIG. 11. $P(T/\langle T\rangle)$ of simulations in Figure 9 (black circles) and the ones with initially $\xi_{\rm back} = 40$ (blue crosses). $\xi_{\rm luck} = 2$ in both cases. The red line denotes the LDM (approach I) with $r_{\rm A} \neq r_k \neq r_{\rm B}$, which is the same simulation as the one in Figure 7.

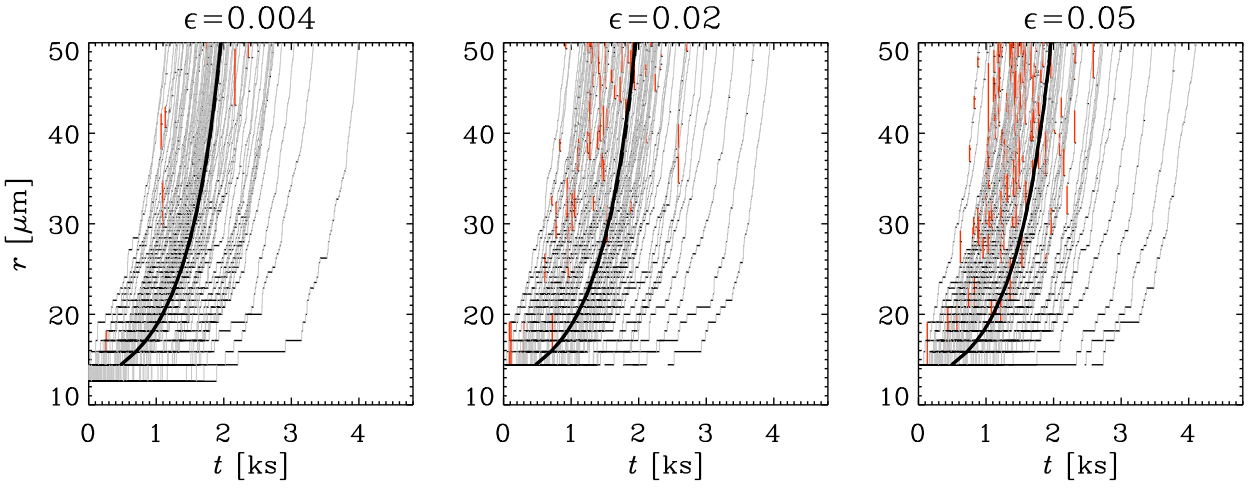

FIG. 12. Growth histories from approach III for $\epsilon = 0.004$ (very few jumps, relevant to the simulations of Figure 7), as well as $\epsilon = 0.02$, and 0.05, where jumps are more frequent. The thick solid line gives the average collision time and cannot be distinguished from that of MFT, which is shown as a thick dotted line.

c. The two aspects of randomness

Let us now quantify the departure that is caused by the use of the Monte Carlo collision scheme. To do this, we need to assess the effects of randomness introduced through equations (3) and (4)

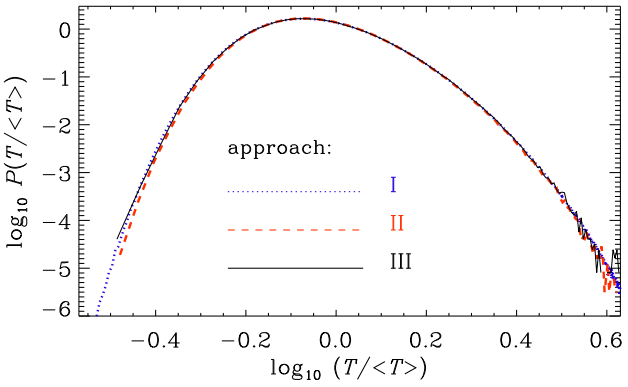

FIG. 13. Comparison of $P(T)$ for approaches I, II, and III.

TABLE 4. Comparison of the moments of $X = \ln(T/\langle T\rangle)$ for approaches I–III.

Approach	$\langle X\rangle$	$\sigma(X)$	skew X	kurt X
I	−0.040	0.279	0.34	0.10
II	−0.039	0.275	0.35	0.11
III	−0.040	0.279	0.34	0.11

on the one hand and the random distribution of the $10\,\mu$m background droplets on the other. Both aspects enter in the superdroplet algorithm.

We recall that in approach II, fluctuations originate solely from the random distribution of the $10\,\mu$m background droplets. In approach III, on the other hand, fluctuations originate solely from the Monte Carlo collision scheme. By contrast, approach I is different from either of the two, because it just uses the exponential distribution of the collision time intervals, which is indirectly reproduced by the random initial droplet distribution in approach II and by the Monte Carlo scheme in approach III.

In Figure 13, we compare approaches I, II, and III. For our solution using approach II, we use a nonperiodic domain of size $10^{-4}\times10^{-4}\times700\,\mathrm{m}^3$, thus containing on average 2100 droplets. This was tall enough for the lucky droplet to reach $50\,\mu$m for all the 10^7 realizations in this experiment. The differences between them are very minor, and also the first few moments are essentially the same; see Table 4. We thus see good agreement between the different approaches. This suggests that the fluctuations introduced through random droplet positions is not crucial and that it can be substituted by the fluctuations of the Monte Carlo scheme alone.

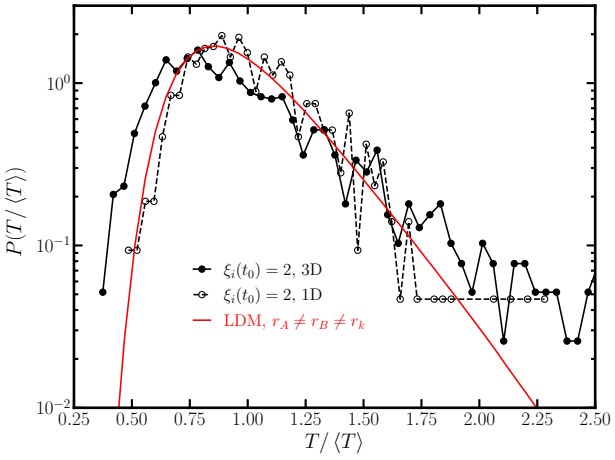

FIG. 14. Comparison of the 3-D case (solid black line) with the 1-D case (dotted black line) with $\xi_i(t_0) = 2$. The red curve shows the result for the LDM approach I with $r_\mathrm{A} \neq r_\mathrm{B} \neq r_k$, which is the same simulation as the one in Figure 7. The 1-D case is the same as the one in Figure 11.

It is worth noting that we were able to perform 10^7 and 10^6 realizations with approaches II and III, respectively, and 10^{10} realizations with approach I, while in the superdroplet algorithm (approach IV), we could only run 10^3–10^4 realizations due to the limitation of the computational power. This may be the reason why fluctuations appear to be slightly underrepresented in the superdroplet algorithm; see Figure 7 and the discussion in section 4.a. Nevertheless, the agreement between the LDM and the superdroplet simulations demonstrates that the superdroplet algorithm does not contain mean-field elements. This can be further evidenced by the fact that the results of approaches II and III agree perfectly with those of approach I, and the superdroplet algorithm is just the combination of approaches II and III.

d. The effects of fluctuations in 3-D simulations

One might have expected that a 3-D simulation could be more realistic and perhaps more accurate than a 1-D simulation. In Figure 14 we compare the resulting $P(T)$ for 3-D and 1-D cases. The result is surprising in that the $P(T)$ curves from the two cases are rather different. The $P(T)$ curve from the 1-D case agrees well with the LDM using approaches I–III. In the 3D case, the fluctuations appear to be vastly exaggerated, similarly to the blue line in Figure 4. This will be discussed next.

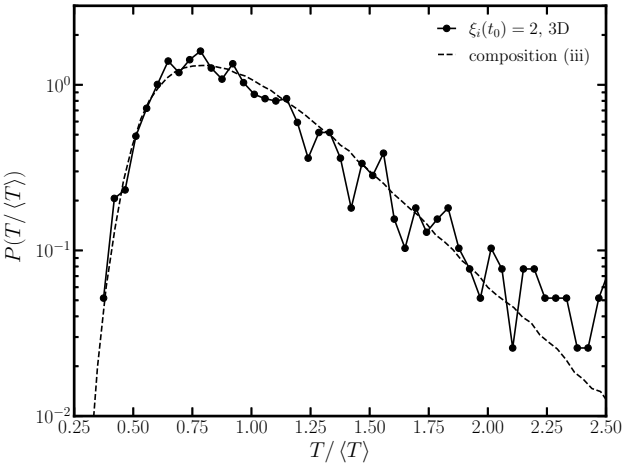

FIG. 15. Comparison between the 3-D superdroplet simulation of Figure 14 and approach II evaluated with a dispersion of $\delta n_{\max}/n_0 = 0.2$, corresponding to composition (iii); see Table A1 for details.

An important difference between 1-D and 3-D is the fact that in 3-D, we accumulate statistics for lucky droplets that fall through vertical columns whose mean droplet number density fluctuates from one column to another. These fluctuations lead to a broadening of $P(T)$, but it is a priori not evident that this explains the 3-D results quantitatively.

In Figure 15, we compare the results from our 3-D superdroplet simulations with the LDM where the relevant fluctuations in droplet number density have been taken into account; see Appendix A3 for details. The lateral fluctuations are quantified by the relative dispersion $\delta n_{\max}/n_0$. We see that there is a close match between the two lines. This suggests that the superdroplet algorithm is accurate and reproduces the results of the LDM, provided all known corrections are applied to it. It also appears that the additional fluctuations introduced in 3-D compensate for the slight underrepresentation of fluctuations in 1-D.

5. Discussion

Fluctuations play a central role in the LDM. We have therefore used it as a benchmark for our simulation. It turns out that the superdroplet algorithm is able to reproduce the growth histories qualitatively and the distribution of cumulative collision times quantitatively. The role of fluctuations was also investigated by Dziekan and Pawlowska (2017), whose approach to assessing the fluctuations is different from ours. Instead of analyzing the distribution of cumulative collision

times, as we do here, their primary diagnostics is the time $t_{10\%}$, after which 10% of the mass of cloud droplets has reached a radius of $40\,\mu$m. In the LDM, such a time would be infinite, because there is only one droplet that is allowed to grow. They then determined the accuracy with which the value of $t_{10\%}$ is determined. The accuracy increases with the square root of the number of physical droplets, provided that the ratio $\xi_i(t_0)$ is kept below a limiting value of about 9. For $\xi_i(t_0) > 9$, they found that there is always a residual error in the value of $t_{10\%}$ that no longer diminishes as they increase the number of physical droplets. We have demonstrated that, when $\xi_i(t_0) > 1$, jumps in the growth history tend to occur. Those jumps can lead to shorter cumulative collision times, which could be the source of the residual error they find.

For a given fraction of droplets that first reach a size of $40\,\mu$m, they also determined their average cumulative collision time. They found a significant dependence on the number of physical droplets. This is very different in our case where we just have to make sure that the number of superdroplets is large enough to keep finding collision partners in the simulations. However, as the authors point out, this is a consequence of them having chosen an initial distribution of droplet sizes that has a finite width. This implies that for a larger number of droplets, there is a larger chance that there could be a droplet that is more lucky than for a model with a smaller number of droplets. In our case, by contrast, we always have a well-known number of superdroplets of exactly $12.6\,\mu$m, which avoids the sensitivity on the number of droplets.

The $\xi_i(t_0) = 9$ limit of Dziekan and Pawlowska (2017) may not be as stringent as originally believed. In this context we need to recall that their criterion for acceptable quality concerned the relative error of the time in which 10% of the total water has been converted to $40\,\mu$m droplets. In our case, we have focussed on the shape of the $P(T)$ curve, especially for small T.

6. Conclusions

We investigated the growth histories of droplets settling in quiescent air using superdroplet simulations. The goal was to determine how accurately these simulations represent the fluctuations of the growth histories. This is important because the observed formation time of drizzle-sized droplets is much shorter than the one predicted based on the mean collisional cross section. The works of Telford (1955), Kostinski and Shaw (2005), and Wilkinson (2016) have shown that this discrepancy can be explained by the presence of stochastic fluctuations in the time intervals

between droplet collisions. By comparing with the lucky droplet model (LDM) quantitatively, we have shown that the superdroplet simulations capture the effect of fluctuations.

A tool to quantify the significance of fluctuations on the growth history of droplets is the distribution of cumulative collision times. Our results show that the superdroplet algorithm reproduces the distribution of cumulative collision times that is theoretically expected based on the LDM. In 3-D, there are additional fluctuations in the system owing to the fact that the mean column density of droplets varies in the horizontal plane. Again, this effect is reproduced by the superdroplet algorithm, where the size distribution is computed from an ensemble with different number densities.

The approximation of representing the dependence of the mean collision rate on the droplet radius by a power law is not accurate and must be relaxed for a useful benchmark experiment. The superdroplet algorithm demonstrates clear differences between 1-D and 3-D simulations. The broader $P(T)$ distribution can be explained by taking variations of the droplet density in the horizontal direction into account.

In summary, the superdroplet algorithm appears to take fluctuations fully into account, at least for the problem of coagulation due to gravitational settling in quiescent air. Computing the distribution of cumulative collision times in the context of turbulent coagulation would be rather expensive, because one would need to perform many hundreds of fully resolved 3-D simulations. Our study suggests that fluctuations are correctly described for collisions between droplets settling in quiescent fluid, but we do not know whether this conclusion carries over to the turbulent case.

Acknowledgments. This work was supported through the FRINATEK grant 231444 under the Research Council of Norway, SeRC, the Swedish Research Council grants 2012-5797, 2013-03992, and 2017-03865, Formas grant 2014-585, by the University of Colorado through its support of the George Ellery Hale visiting faculty appointment, and by the grant "Bottlenecks for particle growth in turbulent aerosols" from the Knut and Alice Wallenberg Foundation, Dnr. KAW 2014.0048. The simulations were performed using resources provided by the Swedish National Infrastructure for Computing (SNIC) at the Royal Institute of Technology in Stockholm and Chalmers Centre for Computational Science and Engineering (C3SE). This work also benefited from computer resources made available through the Norwegian NOTUR program, under award NN9405K. The

source code used for the simulations of this study, the PENCIL CODE, is freely available on `https://github.com/pencil-code/`.

Data availability statement. Datasets for "Collision fluctuations of lucky droplets with superdroplets" (v2021.05.07) are available under `http://10.5281/zenodo.4742786`; see also `http://www.nordita.org/~brandenb/projects/lucky/` for easier access.

APPENDIX

A1. Numerical treatment of approach I

In section b, we noted that solutions to approach I have been obtained with the PENCIL CODE (Pencil Code Collaboration et al. 2021). This might seem somewhat surprising, given that this code is primarily designed for solving partial differential equations. It should be realized, however, that this code also provides a flexible framework for using the message passing interface, data analysis such as the computation of probability density distributions, and input/output.

To compute the probability distribution of T with approach I, we need to sum up sequences of random numbers for many independent realizations of t_k drawn from an exponential distribution. We use the `special/lucky_droplet` module provided with the code. Each point in the computational domain corresponds to an independent realization, so each point is initialized with a different random seed. The domain is divided into 1024 smaller domains, allowing the computational tasks to be performed simultaneously on 1024 processors, which takes about 4 min on a Cray XC40.

A2. Dependence on initial $N_{\rm s}/N_{\rm grid}$ and $N_{\rm d}/N_{\rm s}$

In this appendix, we first test the statistical convergence of $P(T)$ for the initial number of superdroplets per grid cell, $N_{\rm s}(t_0)/N_{\rm grid}$. As discussed in section 2.b, we set $N_{\rm s}(t_0)/N_{\rm grid}=4$ for 1-D simulations. Using the same numerical setup, we examine the statistical convergence of $P(T)$ for different values of $N_{\rm s}(t_0)/N_{\rm grid}$. As shown in Figure A1(a), $P(T)$ converges even at $N_{\rm s}(t_0)/N_{\rm grid}=1$. This is important because one can use as few superdroplets as possible once $N_{\rm grid}$ is fixed, without suffering from the statistical fluctuations.

The most practical application of the superdroplet algorithm is the case when $\xi^i \geq 1$. Thus, we investigate how ξ affects fluctuations by performing the same 1-D simulation as described in

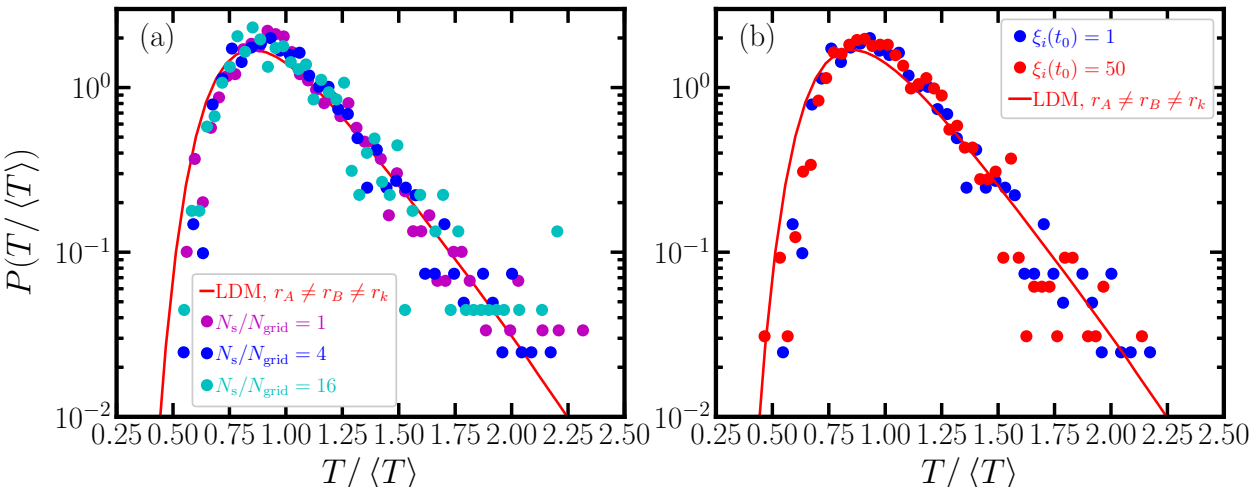

FIG. A1. Comparison of $P(T)$ for (a) different N_s/N_{grid} with fixed $\xi_i(t_0) = 1$ and (b) for different $\xi_i(t_0)$ with fixed $N_s/N_{grid} = 4$. The blue dots represent $P(T/\langle T\rangle)$ from the simulation as in Figure 7. The red curve shows the result for the LDM (approach I) with $r_A \neq r_B \neq r_k$, which is the same simulation as the one in Figure 7.

section 2.b with different values of $\xi^i(t_0)$. Figure A1(b) shows that $P(T)$ is insensitive to $\xi^i(t_0)$, which suggests that the superdroplet algorithm can capture the effects of fluctuations regardless of the value of $\xi^i(t_0)$. This is different from Dziekan and Pawlowska (2017), who found that the approach can represent fluctuations only if $N_d(t_0)/N_s(t_0) \leq 9$.

A3. The 3-D LDM

In this appendix, we describe in more detail the 3-D LDM used in section 4.d. The usual LDM applies to a given value of the number density. Other columns have somewhat different number densities and therefore also different mean cumulative collision times. The LDM with approaches I–III can be extended to include this effect by computing cases with different number densities and then combining $P(T)$ and normalizing by the $\langle T\rangle$ for the combined $P(T)$. This can be formulated by introducing the column density as

$$\Sigma(x, y) = \int_{z_1}^{z_2} n(x, y, z)\, \mathrm{d}z, \tag{A1}$$

where z_1 and z_2 denote the vertical slab in which the first collision occurs, and using this $\Sigma(x, y)$ as a weighting factor for the 1-D distribution functions $P^{1D}(T)$ to compute the 3-D distribution

TABLE A1. Results for approach II using 30,000 realization showing the effects of lateral density fluctuations in 3-D, and comparison with MFT.

Composition	$\delta n_{\rm rms}/n_0$	$\delta n_{\rm max}/n_0$	$T_{\rm min}$ [s]	$T_{\rm MFT}$ [s]	$\langle T\,(n_{\rm max})\rangle$ [s]	$\langle T\rangle$ [s]	$T_{\rm min}/\langle T\rangle$	$T_{P=0.01}/\langle T\rangle$
(0)	0	0	782	1969	2117	2117	0.37	0.44
(i)	0.08	0.10	795	1790	1923	2126	0.37	0.42
(ii)	0.14	0.20	767	1641	1758	2155	0.36	0.40
(iii)	0.20	0.30	631	1515	1628	2203	0.29	0.36

functions as

$$P^{\rm 3D}(T) = \int \Sigma(x,y) P^{\rm 1D}(T)\,{\rm d}x\,{\rm d}y \,\Big/ \int \Sigma(x,y)\,{\rm d}x\,{\rm d}y. \tag{A2}$$

Since the first collision matters the most, we choose $z_2 = z_{\rm max}$ (where the lucky droplet is released) and $z_1 = z_{\rm max} - v_2/\lambda_2$ (where it has its first collision).

Our reference model had a number density of $n_0 = 10^8\,{\rm m}^{-3}$. We now consider compositions of models with different values, where we include the densities (i) $0.9\times10^8\,{\rm m}^{-3}$ and $1.1\times10^8\,{\rm m}^{-3}$, as well as (ii) $0.8\times10^8\,{\rm m}^{-3}$ and $1.2\times10^8\,{\rm m}^{-3}$, and finally also (iii) $0.7\times10^8\,{\rm m}^{-3}$ and $1.3\times10^8\,{\rm m}^{-3}$. All these compositions have the same mean droplet number density but different distributions around the mean. We first average the distribution function and then normalize with respect to the mean collision time for the ensemble over all columns. The parameters of the resulting distributions are listed in Table A1 for three compositions with different density dispersions. We see that, as we move from composition (i) to compositions (ii) and (iii), the dispersion ($\delta n_{\rm rms}/n_0$) increases from 0.08 to 0.14 and 0.20, the distribution $P(T)$ extends further to both the left and right. The reference model is listed as (o). Here we give the rms value of the column-averaged densities, $\langle n\rangle_i$, as

$$\delta n_{\rm rms} = \left[\sum_{i=0}^{N_i}\left(\langle n\rangle_i^2 - n_0^2\right)\right]^{1/2}, \tag{A3}$$

where i denotes the column and N_i is the number of columns. We also give the maximum difference from the average density,

$$\delta n_{\rm max} = \max_i\left(\langle n\rangle_i - n_0\right), \tag{A4}$$

for families (i) with $N_i = 2$, (ii) with $N_i = 4$, and (iii) with $N_i = 6$. We also list in Table A1 several characteristic times in seconds. The quantity $T_{\rm min}$ is the shortest time in which the lucky droplet reaches $50\,\mu$m, $T_{\rm MFT}$ denotes the value based on MFT, $\langle T(n_{\rm max})\rangle$ is the mean value based on the

column with maximum droplet density and $\langle T \rangle$ is the mean based on all columns. It turns out that for the models of all three families, the value of $T_{\min}$ agrees with that obtained solely from the model with the highest density, which is $1.3 \times 10^8\,\mathrm{m}^{-3}$ for composition (ii), for example.

The quantity $\langle T(n_{\max}) \rangle$, i.e., the average time for all of the columns with the largest density, is shorter than the $\langle T \rangle$ for all the columns, especially for composition (iii) where the largest densities occur. For the model (o), there is only one column, so $\langle T(n_{\max}) \rangle$ is the same as $\langle T \rangle$. The value T_{MFT} based on MFT is always somewhat shorter than $\langle T(n_{\max}) \rangle$. Finally, we give in Table A1 the ratios $T_{\min}/\langle T \rangle$ and $T_{P=0.01}/\langle T \rangle$, where the subscript $P = 0.01$ indicates the argument of $P(T)$ where the function value is 0.01.

References

Arabas, A., and S. Shima, 2013: Large-eddy simulations of trade wind cumuli using particle-based microphysics with monte carlo coalescence. *Journal of the Atmospheric Sciences*, **70 (9)**, 2768–2777.

Baehr, H., and H. Klahr, 2019: The concentration and growth of solids in fragmenting circumstellar disks. *The Astrophysical Journal*, **881 (2)**, 162.

Brdar, S., and A. Seifert, 2018: Mcsnow: A monte-carlo particle model for riming and aggregation of ice particles in a multidimensional microphysical phase space. *Journal of Advances in Modeling Earth Systems*, **10 (1)**, 187–206.

Drakowska, J., F. Windmark, and C. P. Dullemond, 2014: Modeling dust growth in protoplanetary disks: The breakthrough case. *Astronomy & Astrophysics*, **567**, A38, 1406.0870.

Dziekan, P., and H. Pawlowska, 2017: Stochastic coalescence in lagrangian cloud microphysics. *Atmospheric Chemistry and Physics*, **17 (22)**, 13 509–13 520.

Dziekan, P., M. Waruszewski, and H. Pawlowska, 2019: University of warsaw lagrangian cloud model (uwlcm) 1.0: a modern large-eddy simulation tool for warm cloud modeling with lagrangian microphysics. *Geoscientific Model Development*, **12 (6)**, 2587–2606.

Gillespie, D. T., 1972: The stochastic coalescence model for cloud droplet growth. *Journal of the Atmospheric Sciences*, **29 (8)**, 1496–1510.

Grabowski, W. W., 2020: Comparison of Eulerian Bin and Lagrangian Particle-Based Microphysics in Simulations of Nonprecipitating Cumulus. *Journal of Atmospheric Sciences*, **77 (11)**, 3951–3970.

Grabowski, W. W., H. Morrison, S.-I. Shima, G. C. Abade, P. Dziekan, and H. Pawlowska, 2019: Modeling of cloud microphysics: Can we do better? *Bulletin of the American Meteorological Society*, **100 (4)**, 655–672.

Hoffmann, F., T. Yamaguchi, and G. Feingold, 2019: Inhomogeneous mixing in lagrangian cloud models: Effects on the production of precipitation embryos. *Journal of the Atmospheric Sciences*, **76 (1)**, 113–133.

Jaruga, A., and H. Pawlowska, 2018: libcloudph++ 2.0: aqueous-phase chemistry extension of the particle-based cloud microphysics scheme. *Geoscientific Model Development*, **11 (9)**, 3623–3645.

Johansen, A., M.-M. Mac Low, P. Lacerda, and M. Bizzarro, 2015: Growth of asteroids, planetary embryos, and kuiper belt objects by chondrule accretion. *Science Advances*, **1 (3)**, e1500 109.

Johansen, A., A. N. Youdin, and Y. Lithwick, 2012: Adding particle collisions to the formation of asteroids and kuiper belt objects via streaming instabilities. *Astron, Astroph.*, **537**, A125.

Kobayashi, H., K. Isoya, and Y. Sato, 2019: Importance of giant impact ejecta for orbits of planets formed during the giant impact era. *The Astrophysical Journal*, **887 (2)**, 226.

Kostinski, A. B., and R. A. Shaw, 2005: Fluctuations and luck in droplet growth by coalescence. *Bull. Am. Met. Soc.*, **86**, 235–244.

Lamb, D., and J. Verlinde, 2011: *Growth by collection*, 380–414. Cambridge University Press.

Li, X.-Y., A. Brandenburg, N. E. L. Haugen, and G. Svensson, 2017: Eulerian and lagrangian approaches to multidimensional condensation and collection. *J. Adv. Modeling Earth Systems*, **9**, 1116–1137.

Li, X.-Y., A. Brandenburg, G. Svensson, N. E. Haugen, B. Mehlig, and I. Rogachevskii, 2018: Effect of turbulence on collisional growth of cloud droplets. *Journal of the Atmospheric Sciences*, **75 (10)**, 3469–3487.

Li, X.-Y., A. Brandenburg, G. Svensson, N. E. Haugen, B. Mehlig, and I. Rogachevskii, 2020: Condensational and collisional growth of cloud droplets in a turbulent environment. *Journal of the Atmospheric Sciences*, **77 (1)**, 337–353.

Li, X.-Y., and L. Mattsson, 2020: Dust growth by accretion of molecules in supersonic interstellar turbulence. *The Astrophysical Journal*, **903 (2)**, 148.

Li, X.-Y., G. Svensson, A. Brandenburg, and N. E. L. Haugen, 2019: Cloud-droplet growth due to supersaturation fluctuations in stratiform clouds. *Atmospheric Chemistry and Physics*, **19 (1)**, 639–648.

Li, X.-Y., and Mattsson, L., 2021: Coagulation of inertial particles in supersonic turbulence. *Astronomy & Astrophysics*, **648**, A52.

Madival, D. G., 2018: Stochastic growth of cloud droplets by collisions during settling. *Theoretical and Computational Fluid Dynamics*, **32 (2)**, 235–244.

Naumann, A. K., and A. Seifert, 2015: A lagrangian drop model to study warm rain microphysical processes in shallow cumulus. *Journal of Advances in Modeling Earth Systems*, **7 (3)**, 1136–1154.

Naumann, A. K., and A. Seifert, 2016: Recirculation and growth of raindrops in simulated shallow cumulus. *Journal of Advances in Modeling Earth Systems*, **8 (2)**, 520–537.

Nesvornỳ, D., R. Li, A. N. Youdin, J. B. Simon, and W. M. Grundy, 2019: Trans-neptunian binaries as evidence for planetesimal formation by the streaming instability. *Nature Astronomy*, **3 (9)**, 808–812.

Onishi, R., K. Matsuda, and K. Takahashi, 2015: Lagrangian tracking simulation of droplet growth in turbulence–turbulence enhancement of autoconversion rate. *Journal of the Atmospheric Sciences*, **72 (7)**, 2591–2607.

Ormel, C., D. Paszun, C. Dominik, and A. Tielens, 2009: Dust coagulation and fragmentation in molecular clouds-i. how collisions between dust aggregates alter the dust size distribution. *Astronomy & Astrophysics*, **502 (3)**, 845–869.

Paoli, R., J. Helie, and T. Poinsot, 2004: Contrail formation in aircraft wakes. *Journal of Fluid Mechanics*, **502**, 361–373.

Pencil Code Collaboration, and Coauthors, 2021: The Pencil Code, a modular MPI code for partial differential equations and particles: multipurpose and multiuser-maintained. *The Journal of Open Source Software*, **6 (58)**, 2807, 2009.08231.

Poon, S. T., R. P. Nelson, S. A. Jacobson, and A. Morbidelli, 2020: Formation of compact systems of super-earths via dynamical instabilities and giant impacts. *Monthly Notices of the Royal Astronomical Society*, **491 (4)**, 5595–5620.

Pruppacher, H. R., and J. D. Klett, 1997: *Microphysics of clouds and precipitation, 2nd edition*. Kluwer Academic Publishers, Dordrecht, The Nederlands, 954p.

Riechelmann, T., Y. Noh, and S. Raasch, 2012: A new method for large-eddy simulations of clouds with lagrangian droplets including the effects of turbulent collision. *New Journal of Physics*, **14 (6)**, 065 008.

Ros, K., and A. Johansen, 2013: Ice condensation as a planet formation mechanism. *Astronomy & Astrophysics*, **552**, A137.

Ros, K., A. Johansen, I. Riipinen, and D. Schlesinger, 2019: Effect of nucleation on icy pebble growth in protoplanetary discs. *Astronomy & Astrophysics*, **629**, A65.

Saffman, P. G., and J. S. Turner, 1956: On the collision of drops in turbulent clouds. *Journal of Fluid Mechanics*, **1**, 16–30.

Saito, I., and T. Gotoh, 2018: Turbulence and cloud droplets in cumulus clouds. *New Journal of Physics*, **20 (2)**, 023 001.

Sato, Y., S.-i. Shima, and H. Tomita, 2017: A grid refinement study of trade wind cumuli simulated by a lagrangian cloud microphysical model: the super-droplet method. *Atmospheric Science Letters*, **18 (9)**, 359–365.

Sato, Y., S.-i. Shima, and H. Tomita, 2018: Numerical convergence of shallow convection cloud field simulations: Comparison between double-moment eulerian and particle-based lagrangian microphysics coupled to the same dynamical core. *Journal of Advances in Modeling Earth Systems*, **10 (7)**, 1495–1512.

Seifert, A., J. Leinonen, C. Siewert, and S. Kneifel, 2019: The geometry of rimed aggregate snowflakes: A modeling study. *Journal of Advances in Modeling Earth Systems*, **11 (3)**, 712–731.

Shima, S., K. Kusano, A. Kawano, T. Sugiyama, and S. Kawahara, 2009: The super-droplet method for the numerical simulation of clouds and precipitation: a particle-based and probabilistic microphysics model coupled with a non-hydrostatic model. *Quart. J. Roy. Met. Soc.*, **135**, 1307–1320, physics/0701103.

Shima, S.-i., Y. Sato, A. Hashimoto, and R. Misumi, 2020: Predicting the morphology of ice particles in deep convection using the super-droplet method: development and evaluation of scale-sdm 0.2. 5-2.2. 0,-2.2. 1, and-2.2. 2. *Geoscientific Model Development*, **13 (9)**, 4107–4157.

Sokal, A., 1997: *Monte Carlo Methods in Statistical Mechanics: Foundations and New Algorithms*. Boston: Springer.

Sölch, I., and B. Kärcher, 2010: A large-eddy model for cirrus clouds with explicit aerosol and ice microphysics and lagrangian ice particle tracking. *Quarterly Journal of the Royal Meteorological Society*, **136 (653)**, 2074–2093.

Telford, J. W., 1955: A new aspect of coalescence theory. *Journal of Meteorology*, **12 (5)**, 436–444.

Twomey, S., 1964: Statistical effects in the evolution of a distribution of cloud droplets by coalescence. *Journal of Atmospheric Sciences*, **21 (5)**, 553–557.

Unterstrasser, S., F. Hoffmann, and M. Lerch, 2017: Collection/aggregation algorithms in lagrangian cloud microphysical models: rigorous evaluation in box model simulations. *Geoscientific Model Development*, **10 (4)**, 1521–1548.

Unterstrasser, S., F. Hoffmann, and M. Lerch, 2020: Collisional growth in a particle-based cloud microphysical model: insights from column model simulations using lcm1d (v1. 0). *Geoscientific Model Development*, **13 (11)**, 5119–5145.

Wilkinson, M., 2016: Large deviation analysis of rapid onset of rain showers. *Physics Review Letter*, **116**, 018 501.

Yang, C.-C., and Z. Zhu, 2020: Morphological signatures induced by dust back reaction in discs with an embedded planet. *Monthly Notices of the Royal Astronomical Society*, **491 (4)**, 4702–4718.

Zannetti, P., 1984: New monte carlo scheme for simulating lagranian particle diffusion with wind shear effects. *Applied Mathematical Modelling*, **8 (3)**, 188–192.

Zsom, A., and C. P. Dullemond, 2008: A representative particle approach to coagulation and fragmentation of dust aggregates and fluid droplets. *Astronomy & Astrophysics*, **489 (2)**, 931–941.

Zsom, A., C. Ormel, C. Güttler, J. Blum, and C. Dullemond, 2010: The outcome of protoplanetary dust growth: pebbles, boulders, or planetesimals?-ii. introducing the bouncing barrier. *Astronomy & Astrophysics*, **513**, A57.